Dynamic Patterns of Gene Regulation I: Simple Two-Gene Systems

Stefanie   Widder
Josef   Schicho
Peter   Schuster

SANTA FE INSTITUTE

Dynamic Patterns of Gene Regulation I: Simple Two Gene Systems

Stefanie Widder[a], Josef Schicho[b], and Peter Schuster[*][a,c]

[a] *Institut für Theoretische Chemie der Universität Wien, Währingerstraße 17, A-1090 Wien, Austria,*

[b] *RICAM – Johann Radon Institute for Computational and Applied Mathematics of the Austrian Academy of Sciences, Altenbergerstraße 69, A-4040 Linz, Austria, and*

[b] *Santa Fe Institute, 1399 Hyde Park Road, Santa Fe, NM 87501, USA*

Abstract: Regulation of gene activities is studied by means of a new computer assisted mathematical analysis of ordinary differential equations (ODEs) derived from binding equilibria and chemical reaction kinetics. Here we present results on cross-regulation of two genes through activator and/or repressor binding. Arbitrary (differentiable) binding function can be used but systematic investigations are presented for gene-regulator complexes with integer valued Hill coefficients up to $n = 4$. The dynamics of gene regulation is derived from bifurcation patterns of the underlying systems of kinetic ODEs. In particular, we present analytical expressions for the parameter values at which one-dimensional (transcritical, saddle-node or pitchfork) and/or two-dimensional (Hopf) bifurcations occur. A classification of regulatory states is introduced, which makes use of he sign of a 'regulatory determinant' D (being the determinant of the block in the Jacobian matrix that contains the derivatives of the regulator binding functions): (i) Systems with $D < 0$, observed, for example, if both proteins are activators or repressors, give rise to one-dimensional bifurcations only and lead to bistability for $n \geq 2$, and (ii) systems with $D > 0$, found for combinations of activation and repression, sustain a Hopf bifurcation and undamped oscillations for $n > 2$. The influence of basal transcription activity on the bifurcation patterns is described. Binding of multiple subunits can lead to richer dynamics than pure activation or repression states if intermediates between the unbound state and the fully saturated DNA initiate transcription. Then, the regulatory determinant D can adopt both signs, plus and minus.

Key words: Basal transcription – bifurcation analysis – cooperative binding – gene regulation – Hill coefficient – Hopf bifurcation.

---

[*]Corresponding author, E-mail: pks@tbi.univie.ac.at

Notation

metabolites	$\mathbf{A}, \mathbf{B}, \mathbf{C}, \ldots,$
concentrations[a] of metabolites	$[\mathbf{A}] = a, [\mathbf{B}] = b, [\mathbf{C}] = c \ldots,$
genes	$\mathbf{G}_1, \mathbf{G}_2,$
concentrations[a] of genes	$[\mathbf{G}_1] = g_1, [\mathbf{G}_2] = g_2,$
transcribed (m)RNAs	$\mathbf{Q}_1, \mathbf{Q}_2,$
concentrations of RNAs	$[\mathbf{Q}_1] = q_1, [\mathbf{Q}_2] = q_2,$
translated proteins	$\mathbf{P}_1, \mathbf{P}_2,$
concentrations[a] of proteins	$[\mathbf{P}_1] = p_1, [\mathbf{P}_2] = p_2,$
gene-protein complexes	$\mathbf{G}_1 \cdot \mathbf{P}_2 = \mathbf{H}_1, \ \mathbf{G}_2 \cdot \mathbf{P}_1 = \mathbf{H}_2,$
concentrations[a] of complexes	$[\mathbf{G}_1 \cdot \mathbf{P}_2] = [\mathbf{H}_1] = h_1,$ $[\mathbf{G}_2 \cdot \mathbf{P}_1] = [\mathbf{H}_2] = h_2,$
dissociation constants	$K_1 = \frac{[\mathbf{G}_2] \cdot [\mathbf{P}_1]}{[\mathbf{H}_2]} = \frac{g_2 \cdot p_1}{h_2},$ $K_2 = \frac{[\mathbf{G}_1] \cdot [\mathbf{P}_2]}{[\mathbf{H}_1]} = \frac{g_1 \cdot p_2}{h_1},$
transcription rate constants	$k_1^{\mathrm{Q}}, k_2^{\mathrm{Q}},$
translation rate constants	$k_1^{\mathrm{P}}, k_2^{\mathrm{P}},$
RNA degradation rate constants	$d_1^{\mathrm{Q}}, d_2^{\mathrm{Q}},$
protein degradation rate constants	$d_1^{\mathrm{P}}, d_2^{\mathrm{P}},$
binding functions	$F_1(p_2), F_2(p_1),$
ratios of rate constants	$\vartheta_1 = \frac{k_1^{\mathrm{Q}} \cdot k_1^{\mathrm{P}}}{d_1^{\mathrm{Q}} \cdot d_1^{\mathrm{P}}}, \ \vartheta_2 = \frac{k_2^{\mathrm{Q}} \cdot k_2^{\mathrm{P}}}{d_2^{\mathrm{Q}} \cdot d_2^{\mathrm{P}}},$ $\phi_1 = \frac{d_1^{\mathrm{P}}}{k_1^{\mathrm{P}}}, \ \phi_2 = \frac{d_2^{\mathrm{P}}}{k_2^{\mathrm{P}}},$
regulatory determinant	$D(p_1, p_2) =$ $= -k_1^{\mathrm{Q}} k_2^{\mathrm{Q}} k_1^{\mathrm{P}} k_2^{\mathrm{P}} \begin{vmatrix} 0 & \left(\frac{\partial F_1}{\partial p_2}\right) \\ \left(\frac{\partial F_2}{\partial p_1}\right) & 0 \end{vmatrix}.$

---

[a]Depending on conditions the symbols express concentrations or activities.

2

Color code for fixed point stability

Condition	Range	Property	Color	Style	Example
$D_{oneD} < D < D_{Hopf}$	low affinity	stable	green	full line	
$D_{oneD} < D < D_{Hopf}$	high affinity	stable	blue	full line	
$D < D_{oneD}$		unstable	red	full line	
$D > D_{Hopf}$		unstable	orange	full line	

Color code for fixed point position

Condition	Range	Color	Coordinate	Style	Example
$D_{oneD} < D < D_{Hopf}$	low affinity	green	$\bar{p}_1$	full line	
			$\bar{p}_2$	broken line	
$D_{oneD} < D < D_{Hopf}$	high affinity	turquoise blue violet	$\bar{p}_1$	full line	
			$\bar{p}_2$	broken line	
$D < D_{oneD}$		red	$\bar{p}_1$	full line	
			$\bar{p}_2$	broken line	
$D > D_{Hopf}$		orange	$\bar{p}_1$	full line	
			$\bar{p}_2$	broken line	

1 Introduction

Theoretical work on gene regulation goes back to the nineteen sixties [1] soon after the first repressor protein had been discovered [2]. A little later the first paper on oscillatory states in gene regulation was published [3]. The interest in gene regulation and its mathematical analysis never ceased [4–6] and saw a great variety of different attempts to design models of genetic regulatory networks that can be used in systems biology for computer simulation of **gen**(etic and met)**abolic** networks.[1] Most models in the literature aims at a minimalist dynamic description which, nevertheless, tries to account for the basic regulatory functions of large networks in the cell in order to provide a better understanding of cellular dynamics. A classic in general regulatory dynamics is the monograph by Thomas and D'Ari [7]. The currently used mathematical methods comprise application of Boolean logic [8–10] stochastic processes [11] and deterministic dynamic models (examples are [12–14]. *In vivo* constructs and selection experiments [15–19] provide insight into regulatory dynamics and better understanding of genabolic networks. Apart from diverse minimalist models [20], relatively few articles are concerned with the mechanistic prerequisites for the occurrence of certain dynamic features based on positive and negative feedback loops [21, 22] like stability, bistability, periodicity or homeostasis. Only few essentially new results are presented in this contribution. Instead we carry out the analytical approach further than in other papers and present a new approach to bifurcation analysis that allows for classification of the dynamical systems for gene regulation.

The basic gene regulation scenario that underlies the calculations presented here is sketched in figure 1 and has been adopted from the booklet by Ptashne & Gann [23]. Two classes of molecular effectors, activators and repressors, decide on the transcriptional activity of a gene, whose activity is classified according to three states: (i) 'Naked' DNA is commonly assumed to have a low or basal transcription activity (basal state), (ii) transcription rises to the normal level when (only) the activator is bound to the regulatory region of the gene (active state), and (iii) complexes with repressor are inactive no matter whether the activator is present or not (inactive state). The basal state is sometimes also characterized as 'leaky transcription'. We shall use this notion here for a general term in the kinetic equations that describes unregulated transcription. Effectors often become active as oligomers, commonly dimers or tetramers, and therefore we shall refer also cases where more than one molecule have to bind before regulation becomes effective (For an overview of mathematical approaches to various binding equilibrium that are of relevance in gene regulation see [24]). The genetic regulatory system is completed by translation of the transcribed mRNAs into protein regulators. Both classes of molecules, mRNAs and proteins, undergo degradation through a first order reaction. DNA, in the form of the genes is assumed to be present at constant concentration. Transcription, translation, and degrada-

---

[1]Discussion and analysis of combined genetic and metabolic networks has become so frequent and intense that we suggest to use a separate term, *genabolic networks* for this class of complex dynamical systems.
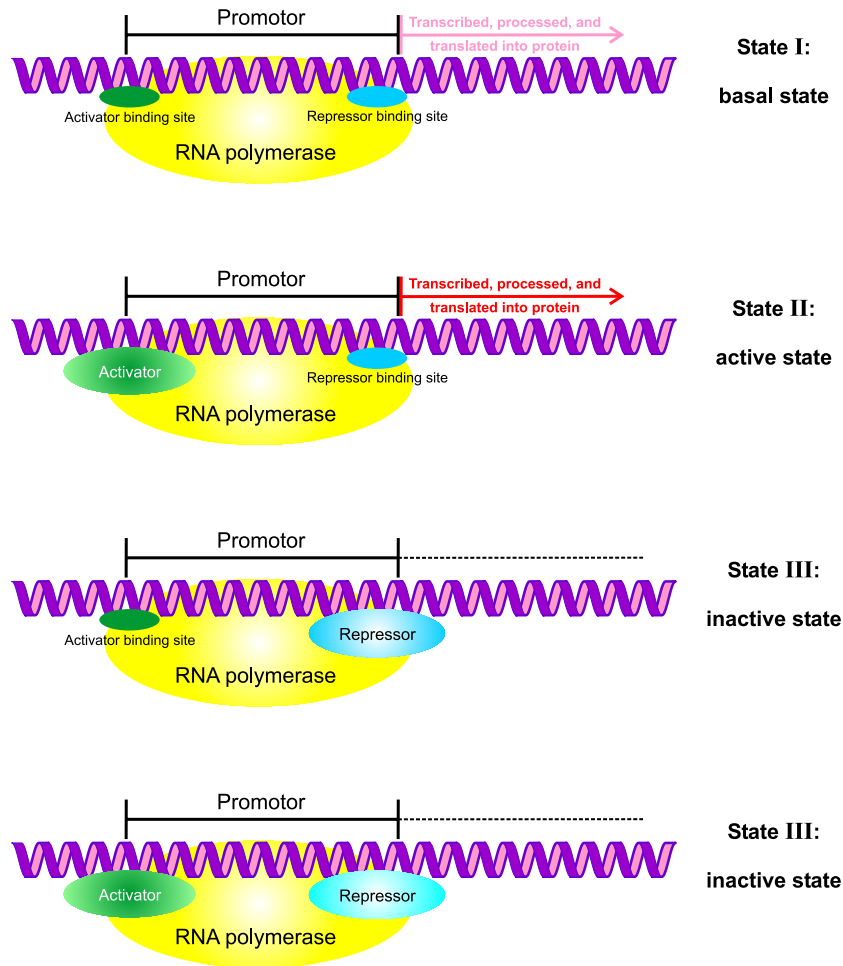
Figure 1: Basic principle of gene regulation. The figure sketches the *regulated recruitment* mechanism of gene activity control in prokaryote cells as discovered with the *lac* genes in *Escherichia coli* [23]. The gene has three states of activity, which are regulated by the presence or absence of glucose and lactose in the medium: State I, **basal state** called 'leaky transcription' occurs when both nutrients are present and it is characterized by low level transcription; neither the activator, the CAP protein, nor the *lac*-repressor protein are bound to their sites on DNA. State II, **activated state** is induced by the absence of glucose and the presence of lactose and then CAP is bound to DNA, but *lac*-repressor protein is absent. Finally, when lactose is absent the gene is in the **inactive state** no matter whether glucose is available or not. Then, the *lac*-repressor protein is bound to DNA and transcription is blocked. The promotor region of the DNA carries specific recognition sites for the RNA polymerase in addition to the binding sites for the regulatory proteins.

tion are multi-step processes and follow rather involved reaction mechanisms. A carefully studied example of such a multi-step process is template-induced RNA synthesis commonly called plus-minus RNA replication [25, 26]. In case monomers and enzyme, the bacteriophage Qβ replicase, are present in excess, the over-all kinetics, however, follows simple first-order rate laws. We shall adopt simple kinetic first order expressions for transcription and translation here.

Following our approach gene regulatory systems can be grouped into two classes: (i) Simple systems for which a complete (computer assisted) qualitative analysis can be carried out analytically,[2] and (ii) complex systems for which qualitative analysis is pending because of hard computational problems or principal difficulties. In both classes the binding function may be arbitrarily complicated provided it is differentiable. The distinction between the two classes is made in section 3.2 by means of the Jacobian matrix of the dynamical systems. In particular, all cross-regulatory two gene systems are of class (i) no matter how sophisticated the binding functions are. In a forthcoming study [27] we shall present analogous results for cases in which the analysis in more involved. These systems include two gene systems where the genes have double functions, for example self-repression and cross-activation, and regulatory systems with more than two genes apart from those with cyclic regulation $(1 \rightarrow 2, 2 \rightarrow 3, \ldots, n \rightarrow 1)$ which fall also into class (i). Here we present the analysis of the ODEs derived from chemical reaction kinetics of gene regulation under the assumption of fast binding equilibria. The (computer assisted) qualitative analysis of the dynamical systems is followed by a discussion of results obtained for some special cases with Hill coefficients $n = 1$, 2, 3, and 4.

2 Kinetic equations

2.1 Binding equilibria

The DNA is assumed to carry two genes, $\mathbf{G}_1$ and $\mathbf{G}_2$, which have binding sites for effectors, activators and/or repressors in the promoter region. Binding of the proteins is assumed to occur fast compared to transcription and translation, and accordingly the equilibrium assumption is valid. The binary interaction is restricted to cross-regulation of the two genes: The translation product of gene $\mathbf{G}_1$ controls the activity of gene $\mathbf{G}_2$ and vice versa. In other words, the activity of gene $\mathbf{G}_1$ is a function of the equilibrium concentration of protein $\mathbf{P}_2$, $\bar{p}_2$, and gene $\mathbf{G}_2$ is likewise controlled by $\mathbf{P}_1$:

$$\mathbf{G}_1 + n_2\,\mathbf{P}_2 \; \xrightleftharpoons{\; g_0\,F_1(\bar{p}_2; n_2, \ldots)\;} \; \mathbf{G}_1 \cdot \mathbf{P}_2 \quad \text{and} \tag{1}$$

$$\mathbf{G}_2 + n_1\,\mathbf{P}_1 \; \xrightleftharpoons{\; g_0\,F_2(\bar{p}_1; n_1, \ldots)\;} \; \mathbf{G}_2 \cdot \mathbf{P}_2 \; . \tag{2}$$

Since the number of DNA molecules is constant, both genes are present in the same total concentrations: $(g_1)_0 = (g_2)_0 = g_0$. In the simplest case,

---

[2]Computer assistance in simple problems may involve computation of solutions for equations but does not require full simulations of regulatory dynamics.

binding equilibria of monomers, $n_1 = n_2 = 1$, and mass action we obtain:[3]

$$\mathbf{G}_1 + \mathbf{P}_2 \; \overset{K_2^{-1}}{\rightleftharpoons} \; \mathbf{G}_1 \cdot \mathbf{P}_2 \quad \text{and} \tag{3}$$

$$\mathbf{G}_2 + \mathbf{P}_1 \; \overset{K_1^{-1}}{\rightleftharpoons} \; \mathbf{G}_2 \cdot \mathbf{P}_1 \,. \tag{4}$$
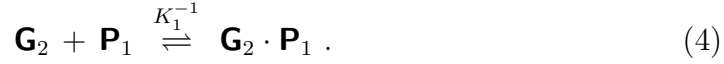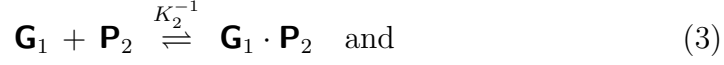
The concentration of the gene protein complex is expressed by

$$[\mathbf{G}_1 \cdot \mathbf{P}_2] \; = \; \bar{c}_1 \; = \; g_0 \cdot \frac{\bar{p}_2}{K_2 + \bar{p}_2} \; \approx \; g_0 \cdot \frac{(\bar{p}_2)_0}{K_2 + (\bar{p}_2)_0}$$

$$[\mathbf{G}_2 \cdot \mathbf{P}_1] \; = \; \bar{c}_2 \; = \; g_0 \cdot \frac{\bar{p}_1}{K_1 + \bar{p}_1} \; \approx \; g_0 \cdot \frac{(\bar{p}_1)_0}{K_1 + (\bar{p}_1)_0} \,,$$

where we approximate the equilibrium protein concentrations by the total concentrations, $\bar{p}_1 \approx (p_1)_0$ and $\bar{p}_2 \approx (p_2)_0$, assuming that the numbers of genes are smaller than the numbers of effector molecules. In order to formulate cross-regulation of two genes in versatile form we generalize the dimensionless regulatory functions, F_j, $j = 1, 2$, to cooperative interactions with arbitrary exponents n (see section 4.2):

$$\text{Gene "1"} \quad \begin{cases} F_1^{(\mathsf{act})}(p_2; K_2, n) \; = \; \frac{p_2^n}{K_2 + p_2^n} & \text{activation,} \\[2mm] F_1^{(\mathsf{rep})}(p_2; K_2, n) \; = \; \frac{K_2}{K_2 + p_2^n} & \text{repression,} \end{cases}$$
$$\text{Gene "2"} \quad \begin{cases} F_2^{(\mathsf{act})}(p_1; K_1, n) \; = \; \frac{p_1^n}{K_1 + p_1^n} & \text{activation,} \\[2mm] F_2^{(\mathsf{rep})}(p_1; K_1, n) \; = \; \frac{K_1}{K_1 + p_1^n} & \text{repression .} \end{cases} \tag{5}$$

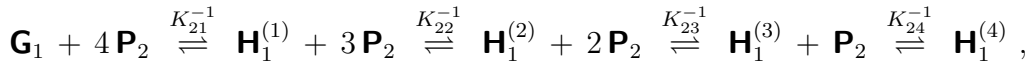Here 'rep' and 'act' stand for repression and activation, respectively, where either the free gene, $\mathbf{G}_j$, or the complex, $\mathbf{G}_j \cdot \mathbf{P}_i$, are transcribed. The exponent n, in particular when determined experimentally, is called the Hill coefficient (See [28] and [29], p. 864 ff.). The Hill coefficient n is related to the molecular binding mechanism. In simple cases n is the number of protein monomers required in binding to the DNA in order to achieve effector activity.

More than one parameter will be required for binding equilibria that involve more than one protein subunit. To give an example, consecutive binding of four ligands $\mathbf{P}_2$ to gene $\mathbf{G}_1$,

$$\mathbf{G}_1 + 4\,\mathbf{P}_2 \; \overset{K_{21}^{-1}}{\rightleftharpoons} \; \mathbf{H}_1^{(1)} + 3\,\mathbf{P}_2 \; \overset{K_{22}^{-1}}{\rightleftharpoons} \; \mathbf{H}_1^{(2)} + 2\,\mathbf{P}_2 \; \overset{K_{23}^{-1}}{\rightleftharpoons} \; \mathbf{H}_1^{(3)} + \mathbf{P}_2 \; \overset{K_{24}^{-1}}{\rightleftharpoons} \; \mathbf{H}_1^{(4)} \,,$$

where $\mathbf{H}_1^{(k)} = \mathbf{G}_1 \cdot (\mathbf{P}_2)_k$, the complex formed by the gene with k protein monomers. If the only complex that is active in transcription were $\mathbf{H}_1^{(4)}$ the binding function would adopt the form[4]

$$F_1^{(\mathsf{act})}(p_2; K_{21}, \ldots, K_{24}) \; =$$

$$= \; \frac{p_2^4}{K_{21}K_{22}K_{23}K_{24} + K_{22}K_{23}K_{24}\,p_2 + K_{23}K_{24}\,p_2^2 + K_{24}\,p_2^3 + p_2^4} \,.$$

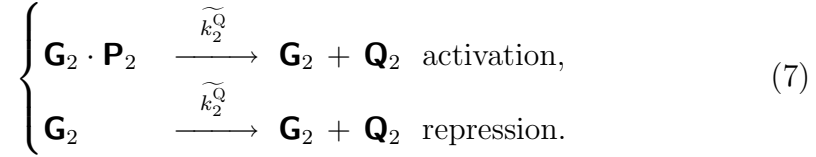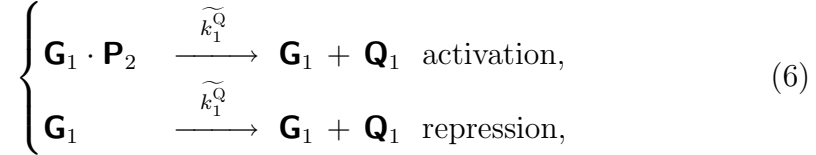[3]It will turn out that the usage of dissociation rather than binding constants is of advantage and therefore we define $K = [\mathbf{G}] \cdot [\mathbf{P}]/[\mathbf{G} \cdot \mathbf{P}]$.

[4]The equilibrium constants applied are *macroscopic dissociation constants*. For equivalent microscopic constants the individual terms in the denominator receive the binomial coefficients, $(1, 4, 6, 4, 1)$, as factors.

Examples of different binding functions will be discussed together with the results derived for the individual systems.
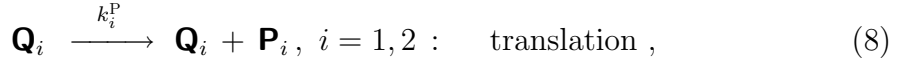
2.2 Reaction kinetics

The transcription reactions come in two variants, an activating mode (corresponding to state II of figure 1) and a repressing mode (corresponding to state III of figure 1). The basal state (state I) can be included in the activating or the repressing mode as we shall see later. The kinetic reaction mechanism for transcription then has the following form:

$$
\begin{cases}
\mathbf{G}_1 \cdot \mathbf{P}_2 \xrightarrow{\widetilde{k_1^{\mathrm{Q}}}} \mathbf{G}_1 + \mathbf{Q}_1 \quad \text{activation,} \\[2mm]
\mathbf{G}_1 \xrightarrow{\widetilde{k_1^{\mathrm{Q}}}} \mathbf{G}_1 + \mathbf{Q}_1 \quad \text{repression,}
\end{cases}
\tag{6}
$$

$$
\begin{cases}
\mathbf{G}_2 \cdot \mathbf{P}_2 \xrightarrow{\widetilde{k_2^{\mathrm{Q}}}} \mathbf{G}_2 + \mathbf{Q}_2 \quad \text{activation,} \\[2mm]
\mathbf{G}_2 \xrightarrow{\widetilde{k_2^{\mathrm{Q}}}} \mathbf{G}_2 + \mathbf{Q}_2 \quad \text{repression.}
\end{cases}
\tag{7}
$$

In case of activation, the regulator-gene complexes are transcribed, whereas the complexes are inactive in repression and transcription is mediated by the free genes.

In contrast to DNA, the transcription products, the mRNAs $\mathbf{Q}_1$ and $\mathbf{Q}_2$, as well as the regulators, the proteins $\mathbf{P}_1$ and $\mathbf{P}_2$, have only finite lifetime because of decay reactions. For translation of mRNAs and for degradation of mRNAs as well as proteins we find:

$$
\mathbf{Q}_i \xrightarrow{k_i^{\mathrm{P}}} \mathbf{Q}_i + \mathbf{P}_i \,, \ i = 1, 2 : \quad \text{translation },
\tag{8}
$$

$$
\mathbf{Q}_i \xrightarrow{d_i^{\mathrm{Q}}} 0 \,, \ i = 1, 2 : \quad \text{degradation , and}
\tag{9}
$$

$$
\mathbf{P}_i \xrightarrow{d_i^{\mathrm{P}}} 0 \,, \ i = 1, 2 : \quad \text{degradation .}
\tag{10}
$$

Translation and degradation reactions are modelled as simple single step processes. The approximation for translation is well justified in case of excess monomers, ribosomes and other translation factors (as mentioned in the introduction). Simple degradation reactions are always of first order. Since the total concentration of the genes is constant and since we shall apply only binding functions that are proportional to g_0, we can absorb the DNA concentration in the rate constant for transcription: $k_i^{\mathrm{Q}} = \widetilde{k_i^{\mathrm{Q}}} \cdot g_0$. As a consequence the rate parameters have different dimensions, $[k_i^{\mathrm{Q}}] = [m \times t^{-1}]$ and $[k_i^{\mathrm{P}}] = [d_i^{\mathrm{Q}}] = [d_i^{\mathrm{P}}] = [t^{-1}]$ where m stands for 'molar' and t stands for 'time'. These substitutions are advantageous in a second aspect, too: The regulatory functions are dimensionless, no matter whether we are using simple hyperbolic or higher order binding equilibria.

Now, we are in a position to write down the kinetic differential equations

for all four molecular species, $\mathbf{Q}_1$, $\mathbf{Q}_2$, $\mathbf{P}_1$, and $\mathbf{P}_2$, derived from two genes:

$$\frac{dq_i}{dt} = \dot{q}_i = k_i^{\text{Q}} F_i(p_j) - d_i^{\text{Q}} q_i \,, \;\; i = 1,2 \,, \;\; j = 2,1 \,, \;\;\; \text{and} \qquad (11)$$

$$\frac{dp_i}{dt} = \dot{p}_i = k_i^{\text{P}} q_i - d_i^{\text{P}} p_i \,, \;\; i = 1,2 \,. \qquad (12)$$

Accordingly, the dynamical system contains eight kinetic parameters and two binding functions. Except for the binding functions $F_i(p_j)$ the system is linear. This property will be important for analyzing the Jacobian matrix and determining the stability of stationary points.

3 Qualitative analysis

3.1 Determination of stationary points

In order to derive equations for the stationary or fixed points of the dynamical system (11,12) we introduce four ratios of reaction rate parameters,

$$\vartheta_i = \frac{k_i^{\text{Q}} k_i^{\text{P}}}{d_i^{\text{Q}} d_i^{\text{P}}} \;\; \text{and} \;\; \phi_i = \frac{d_i^{\text{P}}}{k_i^{\text{P}}} \,, \;\; i = 1,2 \,, \qquad (13)$$

that simplify the expressions obtained from $\dot{q}_i = \dot{p}_i = 0 \,, i = 1,2$:

$$\bar{p}_i - \vartheta_i F_i(\bar{p}_j) = 0 \,, \;\; i = 1,2 \,, \;\; j = 2,1 \,. \qquad (14)$$

The binding functions are normalized $0 \le F_i \le 1$ and hence the equilibrium concentrations of proteins are confined to values in the range $0 \le \bar{p}_i \le \vartheta_i$ with $i = 1,2$. Commonly, the binding functions F_i are ratios of two polynomials and then, equation (14) can always be transformed into two coupled polynomials. Examples will be given in the forthcoming sections. Provided the stationary values of the protein concentrations are known we find for the mRNAs

$$\bar{q}_i = \phi_i \bar{p}_i \,, \;\; i = 1,2 \,. \qquad (15)$$

Again we point at a difference in dimensions: $[\vartheta_i] = [m]$, whereas the ϕ_i's are dimensionless. Stationary concentrations are completely defined by the two ratios of kinetic constants, ϑ_1 and ϑ_2 (and, of course, by the parameters in the functions F_1 and F_2). According to equation (15) the stationary mRNA concentrations $\bar{q}_i$ are related to the corresponding protein concentrations $\bar{p}_i$ through multiplication by a positive factor and hence $\bar{q}_i$ is zero if and only if $\bar{p}_i = 0$.

Apart from an initial phase determined largely by the choice of the initial values $q_i(0), p_i(0)$ ($i = 1,2$) the projection of the trajectories $\big(q_1(t), q_2(t), p_1(t), p_2(t)\big)$ onto the (q_1, q_2)-subspace shows close similarity to that onto the (p_1, p_2)-plane. For stability analysis it is sufficient therefore to consider the fixed points and their properties on either of the two subspaces. We choose the 'protein'-subspace, $\mathcal{P} = \{p_i; p_i \ge 0 \,\forall\, i = 1,2\}$ since protein concentrations are calculated more directly. It is worth noticing that the positions of the stationary points, $\bar{P} = (\bar{p}_1, \bar{p}_2) \in \mathcal{P}$, depend only on ϑ_1 and

Table 1: Protein concentrations in the strong and weak binding limits.

The limits were calculated from equations (17-19) by taking the limits $\lim K_1 \to 0$ and/or $\lim K_2 \to 0$ or $\lim K_1 \to \infty$ and/or $\lim K_2 \to \infty$, respectively.

System	Strong binding: $\lim K_j \to 0$			Weak binding: $\lim K_j \to \infty$		
	j	$\bar{p}_1$	$\bar{p}_2$	j	$\bar{p}_1$	$\bar{p}_2$
act-act[a]	1	0 $\vartheta_1 \frac{\vartheta^n}{K_2+\vartheta_2^n}$	0 ϑ_2	1	0	0
	2	0 ϑ_1	0 $\vartheta_2 \frac{\vartheta^n}{K_1+\vartheta_1^n}$	2	0	0
	1,2	0 ϑ_1	0 ϑ_2	1,2	0	0
act-rep	1	0	0	1	$\vartheta_1 \frac{\vartheta_2^n}{K_2+\vartheta_2^n}$	ϑ_2
	2	ϑ_1	$\vartheta_2 \frac{K_1}{K_1+\vartheta_1^n}$	2	0	ϑ_2
	1,2	0	0	1,2	0	ϑ_2
rep-rep	1	ϑ_1	0	1	$\vartheta_1 \frac{K_2}{K_2+\vartheta_2^n}$	ϑ_2
	2	0	ϑ_2	2	ϑ_1	$\vartheta_2 \frac{K_1}{K_1+\vartheta_1^n}$
	1,2	ϑ_1 0 0	0 0 ϑ_2	1,2	ϑ_1	ϑ_2

[a] The solution $(\bar{p}_1 = 0, \bar{p}_2 = 0)$ is a double root in the strong binding limit.

ϑ_2 and not on all eight kinetic parameters. Substitution of $\bar{p}_2 = \vartheta_2 F_2(\bar{p}_1)$ yields the solution:

$$\bar{p}_1 - \vartheta_1 F_1\Big(\vartheta_2 F_2(\bar{p}_1)\Big) = 0 . \tag{16}$$

Equation (16) leads to high order polynomials for nonlinear binding functions which, nevertheless, are computed straightforwardly for general n for the simple binding functions (5). For activation-activation, activation-repression,

and repression-repression, we obtain

$$\bar{p}_1 \cdot \left(\bar{p}_1^{n \cdot n} \vartheta_2^n - \bar{p}_1^{n \cdot n - 1} \vartheta_1 \vartheta_2^n + K_2 \cdot \sum_{k=0}^{n} \bar{p}_1^{n \cdot (n-k)} \binom{n}{k} K_1^k \right) = 0 \,, \tag{17}$$

$$K_2 \cdot \left(\sum_{k=0}^{n} \bar{p}_1^{n \cdot (n-k)+1} \binom{n}{k} K_1^k \right) + (\bar{p}_1 - \vartheta_1) \cdot (\vartheta_2 K_1)^n = 0 \,, \quad \text{and} \tag{18}$$

$$(\bar{p}_1 - \vartheta_1) \cdot K_2 \cdot \left(\sum_{k=0}^{n} \bar{p}_1^{n \cdot (n-k)} \binom{n}{k} K_1^k \right) + \bar{p}_1 \cdot (\vartheta_2 K_1)^n = 0 \,, \tag{19}$$

respectively. The equilibrium concentration $\bar{p}_2$ is readily obtained from

$$\bar{p}_2 = \frac{\vartheta_2 \cdot \bar{p}_1^n}{K_1 + \bar{p}_1^n} \quad \text{for (17)} \quad \text{and} \quad \bar{p}_2 = \frac{\vartheta_2 \cdot K_1}{K_1 + \bar{p}_1^n} \quad \text{for (18) and (19)}.$$

From equation (17) follows that the origin is always a fixed point for activation-activation systems, $\bar{P}_1 = (0,0)$, corresponding to both genes silenced. The degree of the polynomials in $\bar{p}_1$, $\pi_n = n^2 + 1$, increases with the square of the Hill coefficient and thus reaches already 17 for $n = 4$. Nevertheless, we obtained never more than three or four real roots through numerical solution (for $n \leq 4$). Obviously, we have an even number of real roots for n odd (1 and 3), and an odd number of real roots for n even (2 and 4).

The high degree of the polynomials is prohibitive for direct calculations based on the equations (17-19) but the expressions are suitable to compute, for example, the limits of the equilibrium concentrations for strong and weak binding, $\lim K_{1,2} \to 0$ and $\lim K_{1,2} \to \infty$, respectively. The results are show in table 1 and they correspond completely to the expectations. In case the limits are taken for both constants simultaneously the limiting concentrations are independent of the Hill coefficient n – not unexpectedly since all functions $F_i(\bar{p}_j; K_j, n)$ approach either zero or one in these limits. Examples of individual dynamical systems will be discussed in section 4 and therefore we mention only one general feature here: In the strong binding limit the combination activation-activation leads to two active genes or two silencing of both genes, whereas we have alternate activities – '1' active and '2' silent or '1' silent and '2' active – in the repression-repression system. Weak binding, on the other hand, silences the genes in the **act-act** case and leads to full activities in **rep-rep** systems.

In the next subsection 3.2 we shall make use again of equations (17-19) and derive limits of functions for the strong binding case, which are applied to the analysis of the regulatory dynamics in parameter space.

3.2 Jacobian matrix

The dynamical properties of the ODEs (11,12) are analyzed by means of the Jacobian matrix and its eigenvalues. For the combined vector of all variables, $\mathbf{x} = (x_1, \ldots, x_4) = (q_1, q_2, p_1, p_2)$, the Jacobian matrix A has a useful block
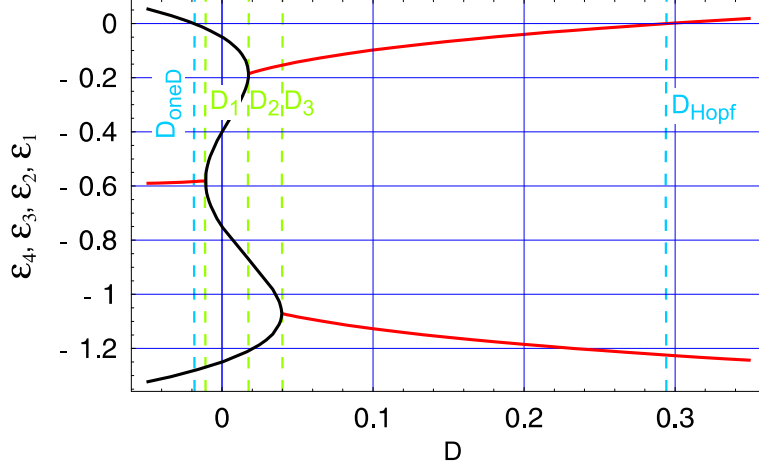
Figure 2: Eigenvalues of the Jacobian matrix (20)**.** The four eigenvalues of a two-gene system, ε_1, ε_2, ε_3, and ε_4, are plotted as functions of D around the point $D = 0$ as reference. The dimension of the ordinate axis is reciprocal time, $[t^{-1}]$. At $D = 0$ and different values of d_1^Q, d_2^Q, d_1^P and d_2^P we observe four negative real eigenvalues of the Jacobian, which are turning into complex conjugate pairs at the values $D = D_1$, $D = D_2$, and $D = D_3$. At D_{oneD} and at D_{Hopf} the fixed point changes stability. The one dimensional bifurcation lies at negative values of D since $D_{\mathsf{oneD}} < 0$, whereas $D_{\mathsf{Hopf}} > 0$, and thus the Hopf bifurcation appears always at positive D-values. Color code: Real eigenvalues are drawn in black and the real parts of complex conjugate pairs of eigenvalues are shown as red lines.

structure:

$$
A = \left\{ a_{ij} = \frac{\partial \dot{x}_i}{\partial x_j} \right\} = \left(\begin{array}{c:c} Q_D & Q_K \\ \hdashline P_K & P_D \end{array} \right) =
$$

$$
= \left(\begin{array}{cc:cc}
-d_1^Q & 0 & k_1^Q \frac{\partial F_1}{\partial p_1} & k_1^Q \frac{\partial F_1}{\partial p_2} \\
0 & -d_2^Q & k_2^Q \frac{\partial F_2}{\partial p_1} & k_2^Q \frac{\partial F_2}{\partial p_2} \\
\hdashline
k_1^P & 0 & -d_1^P & 0 \\
0 & k_2^P & 0 & -d_2^P
\end{array} \right) . \qquad (20)
$$

This block-structure of matrix A largely facilitates the computation of the $2n$ eigenvalues [30, 31]. Since the matrices Q_D and P_K commute, $Q_D \cdot P_K = P_K \cdot Q_D$, the relation

$$
\left| \begin{array}{cc} Q_D & Q_K \\ P_K & P_D \end{array} \right| = \left| Q_D \cdot P_D - Q_K \cdot P_K \right|
$$

holds. In certain cases, among them all forms of cross-regulation of two genes and all forms of cyclic pairwise regulation of more than two genes, $\mathbf{G}_n \Rightarrow \mathbf{G}_1 \Rightarrow \mathbf{G}_2 \Rightarrow \cdots \Rightarrow \mathbf{G}_n$ for arbitrary n [27], the secular equation is of

the form:[5]

$$(\varepsilon + d_1^{\mathrm{Q}})(\varepsilon + d_2^{\mathrm{Q}})(\varepsilon + d_1^{\mathrm{P}})(\varepsilon + d_2^{\mathrm{P}}) + D \;=\; 0 \quad \text{with}$$

$$D \;=\; - k_1^{\mathrm{Q}} k_2^{\mathrm{Q}} k_1^{\mathrm{P}} k_2^{\mathrm{P}} \; \Gamma(p_1, p_2) \; . \tag{21}$$

Since D and $\Gamma(p_1, p_2)$ are obtained from the binding functions by calculating the derivatives with respect to the protein concentrations,

$$\Gamma(p_1, p_2) \;=\; - \begin{vmatrix} 0 & \frac{\partial F_1}{\partial p_2} \\ \frac{\partial F_2}{\partial p_1} & 0 \end{vmatrix} \;=\; \frac{\partial F_1}{\partial p_2} \cdot \frac{\partial F_2}{\partial p_1} \; , \tag{22}$$

we call D the *regulatory determinant* of the dynamical system. Knowledge of D is sufficient to analyze the stability of fixed points and to calculate the parameter values at the bifurcation points. At $D = 0$ the eigenvalues of the Jacobian are the set of all 4 negative degradation rate constants, $-d_i^{\mathrm{Q}}$ and $-d_i^{\mathrm{P}}$ ($i = 1, 2$), which we assume to be ordered by value: $\varepsilon_1 = - \min\{d_1^{\mathrm{Q}}, d_2^{\mathrm{Q}}, d_1^{\mathrm{P}}, d_2^{\mathrm{P}}\}$ is the largest and $\varepsilon_4 = - \max\{d_1^{\mathrm{Q}}, d_2^{\mathrm{Q}}, d_1^{\mathrm{P}}, d_2^{\mathrm{P}}\}$ is the smallest eigenvalue of A. In the non-degenerate case, i.e. when all degradation rate parameters are different, the eigenvalues correspond to four points on the negative (reciprocal time) axis represented by the ordinate axis in figure 2. For a fixed point $\bar{P} \in \mathcal{P}$ with $D = 0$ this implies asymptotic stability. Non-generic cases with double or multiple real roots at $D = 0$ imply also asymptotic stability, only the analytical continuation yielded one or more complex conjugate pairs of eigenvalues with negative real parts.

Figure 2 shows a plot of the individual eigenvalues as functions of D. All curves together form a quartic equation rotated by $\pi/2$, and the shape of the forth-order polynomial determines the bifurcation pattern. At increasing negative values $D < 0$, i.e. in the negative D-direction in figure 2, the two eigenvalues ε_2 and ε_3 approach each other and, at some point, $D = D_1$ this pair of real eigenvalues merges and becomes a complex conjugate pair of eigenvalues. The largest and the smallest eigenvalue, ε_1 and ε_4, remain single-valued. Because of the shape of a quartic equation, the largest eigenvalue ε_1 increases and the lowest eigenvalue ε_4 decreases in the negative D-direction. The condition $\varepsilon_1 = 0$ occurs at the position $D = D_{\mathsf{oneD}}$, which is defined by

$$D_{\mathsf{oneD}} \;=\; - d_1^{\mathrm{Q}} \cdot d_2^{\mathrm{Q}} \cdot d_1^{\mathrm{P}} \cdot d_2^{\mathrm{P}} \; . \tag{23}$$

Here, the fixed point $\bar{P}\big(\bar{p}_1(D), \bar{p}_2(D)\big)$ changes stability and becomes unstable for $D < D_{\mathsf{oneD}}$. Since only one eigenvalue is involved, the corresponding bifurcation is one-dimensional, for example a transcritical, a saddle-node or a pitchfork bifurcation (For examples see section 4). From equation (23) follows the condition for the stability of fixed points with negative D:

$$\bar{P} \text{ with } \Gamma(\bar{p}_1, \bar{p}_2) > 0 \quad \text{is stable iff} \quad \vartheta_1 \cdot \vartheta_2 \cdot \Gamma(\bar{p}_1, \bar{p}_2) \;<\; 1 \; . \tag{24}$$

The stability of fixed points $\bar{P}$ with negative values of D, like their positions $(\bar{p}_1, \bar{p}_2)$, is determined by the two parameter combinations ϑ_1, ϑ_2, and the

---

[5]Generalization to n genes is straightforward: We have $2n$ variables and $2n$ factors rather than four, and the function Γ depends on n protein concentrations.

derivatives of the binding functions (22). For $D < D_{\mathsf{oneD}}$ the fixed point is unstable, and the largest eigenvalue ε_1 is real and positive.

In the direction of positive values, $D > 0$, the eigenvalues approach each other in pairs: $(\varepsilon_1, \varepsilon_2)$ and $(\varepsilon_3, \varepsilon_4)$. If the two eigenvalues in such a pair become equal at some value $D > 0$, at the values D_2 and D_3 in figure 2, the two negative real eigenvalues merge and give birth to a complex conjugate pair with negative real part. The real parts of the two complex conjugate pairs behave like the upper part of a quadratic equation rotated by $\pi/2$ and hence the real part of the pair formed by the two larger eigenvalues, $\lambda_1 = \Re(\varepsilon_1, \varepsilon_2)$, increases with increasing D. As indicated in figure 2 it may cross zero at some point $D = D_{\mathsf{Hopf}}$. There the fixed point looses stability there through a Hopf bifurcation. The value of D can be computed (see the Appendix) and one obtains:

$$
D_{\mathsf{Hopf}} \;=\; \frac{(d_1^{\mathrm{Q}} + d_2^{\mathrm{Q}})(d_1^{\mathrm{Q}} + d_1^{\mathrm{P}})(d_1^{\mathrm{Q}} + d_2^{\mathrm{P}})(d_2^{\mathrm{Q}} + d_1^{\mathrm{P}})(d_2^{\mathrm{Q}} + d_2^{\mathrm{P}})(d_1^{\mathrm{P}} + d_2^{\mathrm{P}})}{(d_1^{\mathrm{Q}} + d_2^{\mathrm{Q}} + d_1^{\mathrm{P}} + d_2^{\mathrm{P}})^2} \;. \quad (25)
$$

If $0 \le D < D_{\mathsf{Hopf}}$ is fulfilled for some fixed point $\bar{P} \in \mathcal{P}$ with positive D, the fixed point is stable:

$$
\bar{P} \text{ with } \Gamma(\bar{p}_1, \bar{p}_2) < 0 \text{ is stable iff } - k_1^{\mathrm{Q}} \cdot k_2^{\mathrm{Q}} \cdot k_1^{\mathrm{P}} \cdot k_2^{\mathrm{P}} \cdot \Gamma(\bar{p}_1, \bar{p}_2) < D_{\mathsf{Hopf}}. \quad (26)
$$

$\bar{P}$ is unstable for $D > D_{\mathsf{Hopf}}$, and at $D = D_{\mathsf{Hopf}}$ we expect a marginally stable point with concentric orbits in a (small) neighborhood of $\bar{P}$. In summary, all fixed points $\bar{P} \in \mathcal{P}$ are asymptotically stable in the range $D_{\mathsf{oneD}} < D < D_{\mathsf{Hopf}}$ (see the Appendix), all four eigenvalues are real between $D_1 < D < D_2$.

Equation (21) can be solved easily if all degradation rate parameters are equal, $d_1^{\mathrm{Q}} = d_n^{\mathrm{Q}} = d_1^{\mathrm{P}} = d_2^{\mathrm{P}} = d$:

$$
(\varepsilon + d)^4 + D \;=\; 0 \quad \Longrightarrow \quad \varepsilon_i = -d + \sqrt[4]{-D}\,, \; i = 1, \ldots, 4\,.
$$

Similarly, the eigenvalues are readily calculated if all RNA and all protein degradation rates are the same: $d_1^{\mathrm{Q}} = d_2^{\mathrm{Q}} = d^{\mathrm{Q}}$ and $d_1^{\mathrm{P}} = d_2^{\mathrm{P}} = d^{\mathrm{P}}$ yields

$$
(\varepsilon + d^{\mathrm{Q}})(\varepsilon + d^{\mathrm{P}}) \;=\; \pm\sqrt{-D}\,,
$$

where the computation boils down to solving two quadratic equations.

For a given fixed point the function $\Gamma(\bar{p}_1, \bar{p}_2)$ determines the bifurcation behavior of the system. In all examples with simple binding functions of type (5), $\Gamma(\bar{p}_1, \bar{p}_2)$ is either positive or negative for all (non-negative) values of the concentrations p_1 and p_2. Indeed we find $\Gamma(\bar{p}_1, \bar{p}_2) \ge 0$ for activation of both genes (act-act) and repression of both genes (rep-rep), whereas combinations of activation and repression, (act-rep) and (rep-act), yields always non-positive values, $\Gamma(\bar{p}_1, \bar{p}_2) \le 0$. According to (21) D has opposite sign to Γ. Calculation of the regulatory determinant for arbitrary n is straightforward and yields:

$$
D \;=\; \mp k_1^{\mathrm{Q}} k_2^{\mathrm{Q}} k_1^{\mathrm{P}} k_2^{\mathrm{P}} \, \frac{n^2 K_1 K_2 \, \bar{p}_1^{n-1} \bar{p}_2^{n-1}}{(K_1 + \bar{p}_1^n)^2 (K_2 + \bar{p}_2^n)^2} \;. \quad (27)
$$

Here, the minus sign holds for act-act and rep-rep whereas the plus sign is true for act-rep and rep-act. In case of act-act insertion of the coordinates of

the fixed point at the origin, $\bar{P}_1 = (0,0)$, yields the very general result that $\bar{P}_1$ is always stable for $n \geq 2$, because we obtain $D = 0$ in this case.

Equations (17-19) are useful in searching parameter space for bifurcations. Auxiliary variables can be used to define manifolds on which the search is carried out. As an illustrative example we consider the search for a Hopf bifurcation along the one-dimensional manifold defined by ($k_1^Q = \chi_1 \cdot s$, $k_2^Q = \chi_2 \cdot s, K_1 = \lambda_1/s, K_2 = \lambda_2/s$) in the act-rep system (18). From these relations follows $\vartheta_i = \delta_i \cdot s$ with $\delta_1 = \left(k_1^P/(d_1^Q d_1^P)\right)\chi_1$ and $\delta_2 = \left(k_2^P/(d_2^Q d_2^P)\right)\chi_2$, respectively. The computation of the equilibrium concentrations for large s is straightforward and yields for $n > 1$:

$$\bar{p}_1 = \alpha_1 \cdot s^{2/(n^2+1)} \quad \text{with} \quad \alpha_1 = \left(\frac{\delta_1(\delta_2\lambda_1)^n}{\lambda_2}\right)^{1/(n^2+1)} \quad \text{and}$$

$$\bar{p}_2 = \alpha_2 \cdot s^{-2n/(n^2+1)} \quad \text{with} \quad \alpha_2 = \left(\frac{\lambda_1}{(\delta_1(\delta_2\lambda_1)^{n^3/(n^2+1)}}\right)^{n/(n^2+1)} .$$

Insertion into the expression for the regulatory determinant leads to exact cancellation of the powers of s and we find in the

$$\text{limit of large } s: \quad D_{\text{lim}} \approx k_1^Q k_2^Q k_1^P k_2^P \frac{n^2}{\vartheta_1 \vartheta_2} = d_1^Q d_2^Q d_1^P d_2^P n^2 . \tag{28}$$

This value has to be compared with the condition for the occurrence of a Hopf bifurcation (25). As an example of an application we analyze the function

$$H(d_1^Q, d_2^Q, d_1^P, d_2^P, n) = D_{\text{lim}} \Big/ D_{\text{Hopf}} =$$

$$= n^2 \frac{d_1^Q d_2^Q d_1^P d_2^P (d_1^Q + d_2^Q + d_1^P + d_2^P)^2}{(d_1^Q + d_2^Q)(d_1^Q + d_1^P)(d_1^Q + d_2^P)(d_2^Q + d_1^P)(d_2^Q + d_2^P)(d_1^P + d_2^P)} , \tag{29}$$

to show whether or not act-rep systems with Hill coefficient $n > 1$ can undergo a Hopf bifurcation at certain parameter values and sustain undamped oscillations. A value $H > 1$ indicates that a limit cycle exists for sufficiently large values of s. The maximum of H is computed by partial differentiation with respect to the degradation rate constants[6]

$$\left(\frac{\partial H}{\partial d_1^Q}\right) = 0 \implies (d_1^Q)^3(d_2^Q + d_1^P + d_2^P) + (d_1^Q)^2\left((d_2^Q)^2 + (d_1^P)^2 + (d_2^P)^2\right) -$$

$$- 3d_1^Q(d_2^Q d_1^P d_2^P) - d_2^Q d_1^P d_2^P(d_2^Q + d_1^P + d_2^P) = 0 .$$

This cubic equation is hard to analyze but the question raised here can be answered without explicit solution. We assume $d_2^Q = d_1^P = d_2^P = d$ and obtain

$$(d_1^Q - d)(d_1^Q + d)^2 = 0 \implies d_1^Q = d \quad \text{and} \quad H(d,d,d,d,n) = \frac{n^2}{4} .$$

By numerical inspection we showed that any deviation from uniform degradation rate parameters leads to a smaller value for the maximum of H. In

---

[6]Since the function (29) is symmetric with respect to all four rate parameters all four partial derivatives have identical analytical expressions.

the strong binding limit the act-rep system with $n = 2$ is confined to values $H \leq 1$ and indeed no limit cycle has been observed. Systems with $n \geq 3$, however, show values of $H_{\max} = n^2/4 > 1$ in certain regions of parameter space, and they do indeed sustain undamped oscillations. For the fixed point in the positive quadrant the D-value increases from weak to strong binding (See section 4.2) and this completes the arguments for the nonexistence of undamped oscillation for $n = 2$.

3.3 Basal transcription

The basal state shown in figure 1 is often characterized as 'leaky transcription' since it leads to low levels of mRNA. In order to take basal activity formally into account we add (small) constant terms, γ_1 and γ_2, to the binding functions (5) and find for activation and repression

$$
\begin{aligned}
F_1^{(\text{act})}(p_2) &= \gamma_1 + \frac{p_2^n}{K_2 + p_2^n} = \frac{\gamma_1 K_2 + (1 + \gamma_1)p_2^n}{K_2 + p_2^n} \\
F_1^{(\text{rep})}(p_2) &= \gamma_1 + \frac{K_2}{K_2 + p_2^n} = \frac{(1 + \gamma_1)K_2 + \gamma_1 p_2^n}{K_2 + p_2^n} \\
F_2^{(\text{act})}(p_1) &= \gamma_2 + \frac{p_1^n}{K_1 + p_1^n} = \frac{\gamma_2 K_1 + (1 + \gamma_2)p_1^n}{K_1 + p_1^n} \\
F_2^{(\text{rep})}(p_1) &= \gamma_2 + \frac{K_1}{K_1 + p_1^n} = \frac{(1 + \gamma_2)K_1 + \gamma_2 p_1^n}{K_1 + p_2^n} \ .
\end{aligned}
\tag{30}
$$

Basal transcription activity is readily incorporated into the analytic procedure described here. The computation of fixed points is straightforward although it involves more terms. Since the constant terms vanish through differentiation, the regulatory determinant and the whole Jacobian matrix depend on basal transition only via the changes in the positions of the fixed points, $\bar{P} = (\bar{p}_1, \bar{p}_2)$.

For gene regulation leaky transcription is most important in cases where both genes are activated. Activation without basal transcription allows for irreversible silencing of both genes since they can be turned off completely and after degradation of the activator proteins the system cannot recover its activity. In mathematical terms the origin, $\bar{P}(0,0)$, is an asymptotically stable fixed point. Basal transcription changes this situation because some low-level protein synthesis is always going on and the origin is a fixed point no longer. In the forthcoming section we shall consider several examples where leaky transcription has been included.

4 Selected examples

Examples for activation and repression were considered for non-cooperative binding ($n = 1$) as well as for cooperative binding ($n \geq 2$) up to $n = 4$. In addition, examples were included where intermediate complexes are active in transcription. Our calculations have shown that at low ratios ϑ/K all systems sustain asymptotically stable stationary states in the positive quadrant including the origin, all except very few (see table 4) undergo a bifurcation at some larger value of ϑ/K and reach, thereafter, the relevant or *regulated* state. The changes in the dynamical patterns in parameter space are investigated by means of an auxiliary variable s that defines a path in parameter space (See section 3.2). The range in parameter space with low values ϑ/K is characterized by low ratios of reaction rate parameters and/or high dissociation parameters of the regulatory complexes, which is tantamount to low binding constants or low affinities. It will be denoted here as the *unregulated regime*, because the dynamics in this range is not suitable for regulatory functions. In contrast, the parameter range with high ratios ϑ/K above the bifurcation value will be called the *regulated regime* since bistabilities or oscillations (or sometimes both) occur in this region. In the cases discussed here we shall investigate paths through parameter space that lead from the unregulated to the regulated regime which can be achieved, for example, by assuming $\vartheta \propto s$ and $K \propto s^{-1}$.[7] For all pure activation-activation and repression-repression systems the function D is non-positive and hence Hopf bifurcations, and limit cycles derived from them, can be excluded. Instead one dimensional bifurcations, transcritical, saddle-node, and pitchfork bifurcations, are observed, the latter two resulting in bistability of the system. Activation-repression yields non-negative values of D and hence the systems may reach oscillatory states via the Hopf bifurcation mechanism. Examples, where intermediate complexes are active in transcription, were included because they may give rise to regulatory determinants D that can adopt positive as well as negative values and therefore may sustain oscillations and bistability at different parameter values.

4.1 The non-cooperative binding case

In the non-cooperative case binding of effectors to the regulatory regions of DNA is described by the equilibria (3) and (4). As said we have two classes of binding functions (5) and this leads to three different cases: (i) activation-activation, (ii) activation-repression, and (iii) repression-repression, which will be handled separately.

Activation-activation. The binding functions for this case are

$$F_1(p_2) = \frac{p_2}{K_2 + p_2} \quad \text{and} \quad F_2(p_1) = \frac{p_1}{K_1 + p_1} \ . \tag{31}$$

---

[7]Considering the limits, $\lim_{s \to 0} \bar{P}_k(s)$ and $\lim_{s \to \infty} \bar{P}_k(s)$ with $k = 1, 2, \ldots$, is important for all fixed points, for example, in order to recognize equivalent and non-equivalent paths through parameter space.
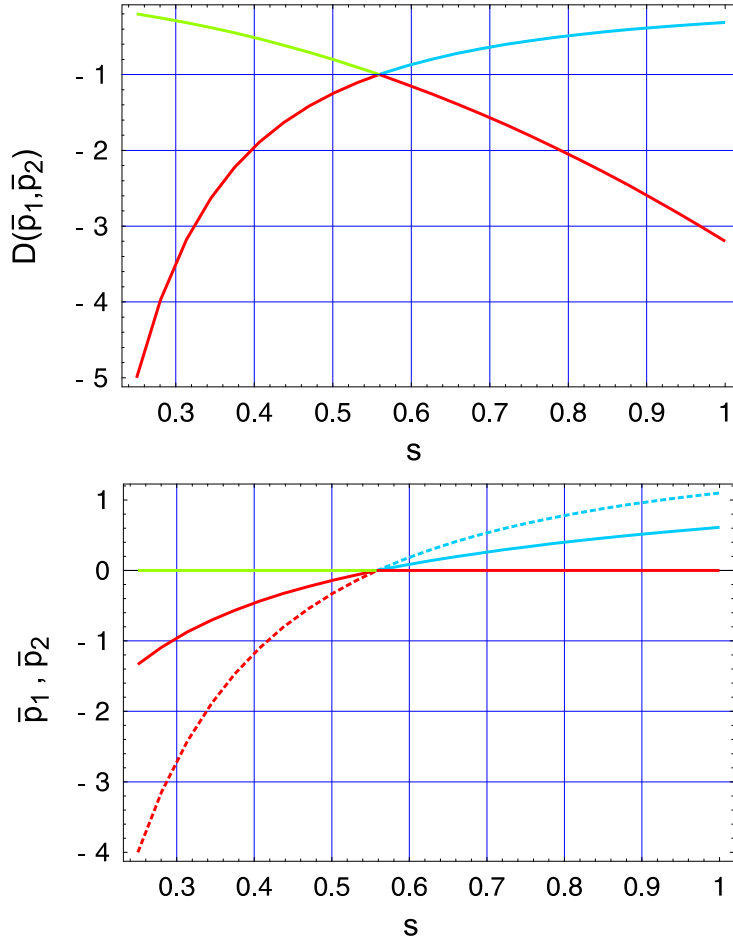
Figure 3: Position and stability of the two fixed points in the two-gene non-cooperative activation-activation system according to equation (32). The upper part of the figure shows the regulatory determinant D as a function of the auxiliary variable s for both fixed points $\bar{P}_1$ and $\bar{P}_2$. According to equation (23) we observe a transcritical bifurcation at the value $s = s_{\mathsf{oneD}} = 0.559$. Both D-functions adopt the value $D_{\mathsf{oneD}} = -1$ and exchange stability at this point. The origin, $\bar{P}_1$, is asymptotically stable for $s < s_{\mathsf{oneD}}$ whereas $\bar{P}_2$ shows stability above this value. The lower plot shows the position of the two fixed points as a function of s. Parameter values: $k_1^{\mathrm{Q}} = k_2^{\mathrm{Q}} = 1$, $K_1 = 0.5/s$, $K_2 = 2.5/s$, $k_1^{\mathrm{P}} = k_2^{\mathrm{P}} = 2$, and $d_1^{\mathrm{Q}} = d_2^{\mathrm{Q}} = d_1^{\mathrm{P}} = d_2^{\mathrm{P}} = 1$. Color code see 'Notation'.

The search for stationary points leads to two solutions:

$$\bar{P}_1 = (0,0) \quad \text{and} \quad \bar{P}_2 = \left(\frac{\vartheta_1 \vartheta_2 - K_1 K_2}{\vartheta_2 + K_2} \,,\, \frac{\vartheta_1 \vartheta_2 - K_1 K_2}{\vartheta_1 + K_1} \right) . \tag{32}$$

For $\vartheta_1 \vartheta_2 > K_1 K_2$ the fixed point $\bar{P}_2$ is inside the positive quadrant of protein space and it is stable as can be readily verified by means of equation (24). At the critical value $\vartheta_1 \vartheta_2 = K_1 K_2$ the two fixed points exchange stability as required for a transcritical bifurcation. A special example is shown in figure 3: The path through parameter space is defined by $K_1 = 0.5/s$ and $K_2 = 2.5/s$ (The other parameters are summarized in the caption of figure 3). The limits for the position of the two fixed points are: (i) $\bar{P}_1$ stays at the origin for all s, and (ii) for $\bar{P}_2$ we compute $\lim_{s \to 0} \bar{P}_2 = (-\infty, -\infty)$ and $\lim_{s \to \infty} \bar{P}_2 = (2, 2)$.
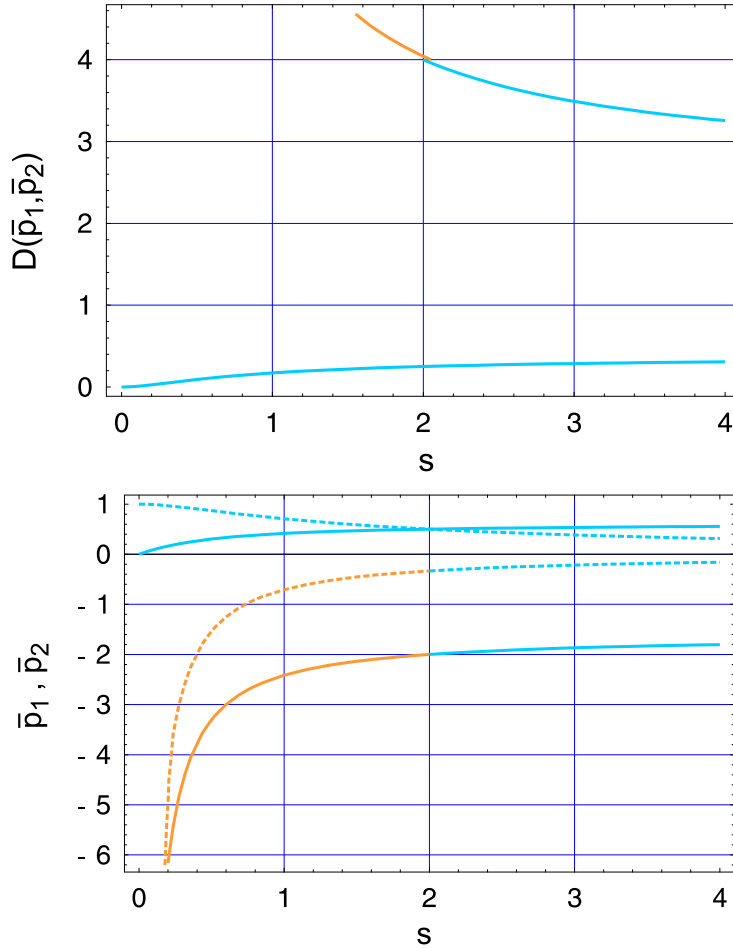
18

Figure 4: Position and stability of the two fixed points in the two-gene non-cooperative activation-repression system. The upper part of the figure shows the regulatory determinant D as a function of the auxiliary variable s for both fixed points $\bar{P}_1$ and $\bar{P}_2$. The lower plot shows the position of the two fixed points as a function of s. The 'non-biological' fixed point $\bar{P}_1$ lies in the negative quadrant, the regulatory determinant $D(\bar{P}_1)$ adopts the value $D = 4$ at $s = 2$ and the system undergoes a Hopf bifurcation there (figure 5). The relevant fixed point $\bar{P}_2$ is asymptotically stable for all values of s. Parameter values: $k_1^{\mathrm{Q}} = k_2^{\mathrm{Q}} = 1$, $K_1 = K_2 = 1/s$, $k_1^{\mathrm{P}} = k_2^{\mathrm{P}} = 2$, and $d_1^{\mathrm{Q}} = d_2^{\mathrm{Q}} = d_1^{\mathrm{P}} = d_2^{\mathrm{P}} = 1$. Color code see 'Notation'.

It is worth considering the physical meaning of the stability condition for $\bar{P}_2$: Since the parameters ϑ are the squares of the geometric means of the formation rate constants divided by the degradation rate constants and the K's are the reciprocal binding constant, both genes are active for sufficiently large formation rate parameters and high binding affinities. The combination activation-activation with non-cooperative binding shows modest regulatory properties. It sustains two states: (i) A regulated state where both genes are transcribed and (ii) a state of 'extinction' with both genes silenced.
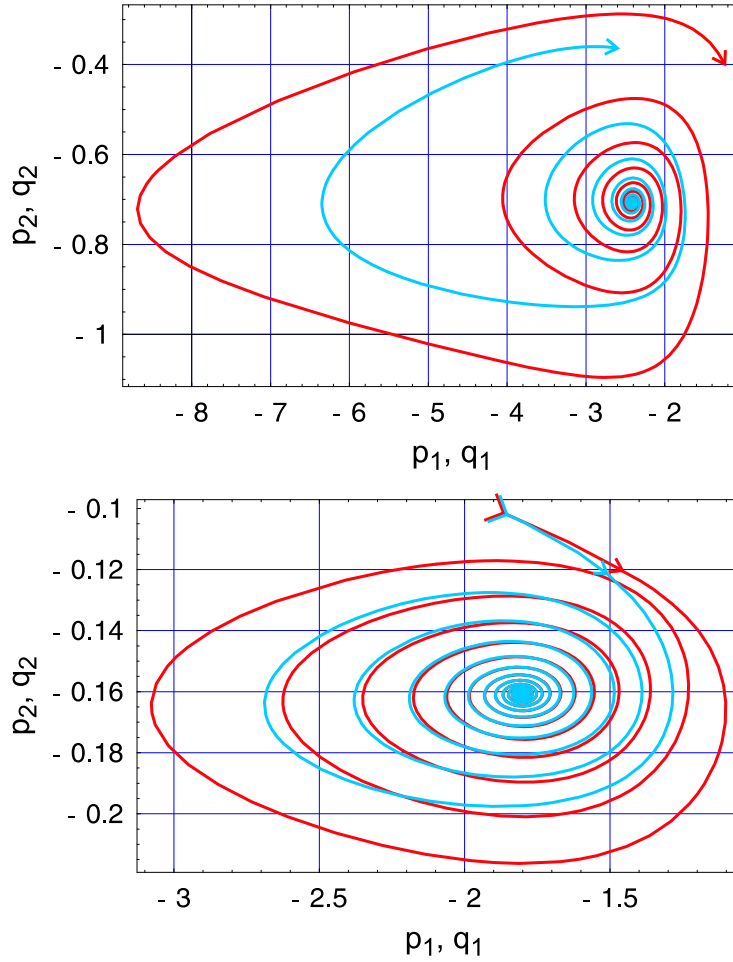
Figure 5: A Hopf bifurcation at $\bar{P}_2$ in the two-gene non-cooperative activation-repression system. From the dependence of the regulatory determinant D at $\bar{P}_1$ on the auxiliary variable s shown in the upper plot of figure 4 a bifurcation with $D = 4$ is expected to occur at the value $s = 2$. We show trajectories for $s = 1$ (upper plot; all parameter values identical with the choice in figure 4) and $s = 4$ (lower plot) and observe spiralling out and spiralling in, respectively. Color code: The projection of the trajectory onto the mRNA concentration subspace, $\big(q_1(t), q_2(t)\big)$, is shown in red and the projection onto protein subspace, $\big(p_1(t), p_2(t)\big)$ is plotted in blue.

Activation-repression   For activation of gene one and repression of gene two the binding functions are of form:

$$F_1(p_2) = \frac{p_2}{K_2 + p_2} \quad \text{and} \quad F_2(p_1) = \frac{K_1}{K_1 + p_1} \ . \tag{33}$$

Here the stationary conditions sustain two fixed points that are obtained as solutions of the quadratic equation

$$K_2 \bar{p}_1^2 + (\vartheta_2 + K_2) K_1 \bar{p}_1 - \vartheta_1 \vartheta_2 K_1 = 0 \ .$$

This equation has one positive and one negative solution for $\bar{p}_1$. For known $\bar{p}_1$ the second protein concentration is calculated from

$$\bar{p}_2 = \frac{\vartheta_2 K_1}{K_1 + \bar{p}_1} \ .$$

20

Combining this equation with $\bar{p}_1 = \vartheta_1 \bar{p}_2 / (K_2 + \bar{p}_2)$ allows to prove that both variables, $\bar{p}_1$ and $\bar{p}_2$, have the same sign and accordingly, one fixed point, $\bar{P}_1$ lies inside the negative quadrant of the (p_1, p_2)-space and plays no role in biology. The second stationary point is characterized by two positive concentration values, lies inside the positive quadrant, and is stable (figure 4).

The properties of the fixed point $\bar{P}_1$ are, nevertheless, useful for the analysis of the dynamical system in the sense of continuation into the neighboring quadrants. In particular, it allows for an inspection of the condition (26). Differentiation shows that the function $D(p_1, p_2)$ of equation (21) is always positive and then the observation of a Hopf bifurcation cannot be excluded. In the example shown in figure 4 $D(\bar{P}_1)$ adopts indeed the value $D = 4$ at $\bar{P}_1$ (for the auxiliary parameter $s = 2$). As shown in figure 5 the trajectories change from spiralling in at $s = 4$ to spiralling out at $s = 1$. For careful parameter choices a small limit cycle is observed further apart from the (unstable) fixed point the trajectories of the dynamical system diverges when they come close to the lines $p_1 = -K_1$ and $p_2 = -K_2$.

In summary we obtain only the scenario of the unregulated regime and no bifurcation to a state that is interesting from the point of regulation. The system is characterized by a single state, which is stable for all physical parameter values, and shows no potential regulatory properties.

Repression-repression. Both genes code for repressors in the third scenario. The binding functions are of the form

$$F_1(p_2) \;=\; \frac{K_2}{K_2 + p_2} \quad \text{and} \quad F_2(p_1) \;=\; \frac{K_1}{K_1 + p_1} \;, \tag{34}$$

and the two stationary solutions are again obtained as solutions of a quadratic equation,

$$K_2 \, \bar{p}_1^2 \;+\; (\vartheta_2 K_1 - \vartheta_1 K_2 + K_1 K_2) \, \bar{p}_1 \;-\; \vartheta_1 \, K_1 \, K_2 \;=\; 0 \;,$$

and the same relation as in the previous section

$$\bar{p}_2 \;=\; \frac{\vartheta_2 \, K_1}{K_1 + \bar{p}_1} \;.$$

Similar as in the previous example it can be shown that $\bar{p}_1$ and $\bar{p}_2$ have always the same sign. One of the two solutions is unstable and lies in the negative quadrant whereas the other one, the physically meaningful solution, is situated in the positive quadrant and it is asymptotically stable (figure 6). The observed stabilities are readily predicted from inspection of equation (21): Since D is non-positive we have either four real negative eigenvalues or two real eigenvalues and a complex conjugate pair with a real part lying between the other two (figure 2). The stable fixed point is identified by $0 \geq D \geq -1$, the unstable one by $D < -1$.

In the non-cooperative binding case the combination repression-repression gives rise to a single state only, it represents the unregulated scenario, and it is not suitable for regulation.
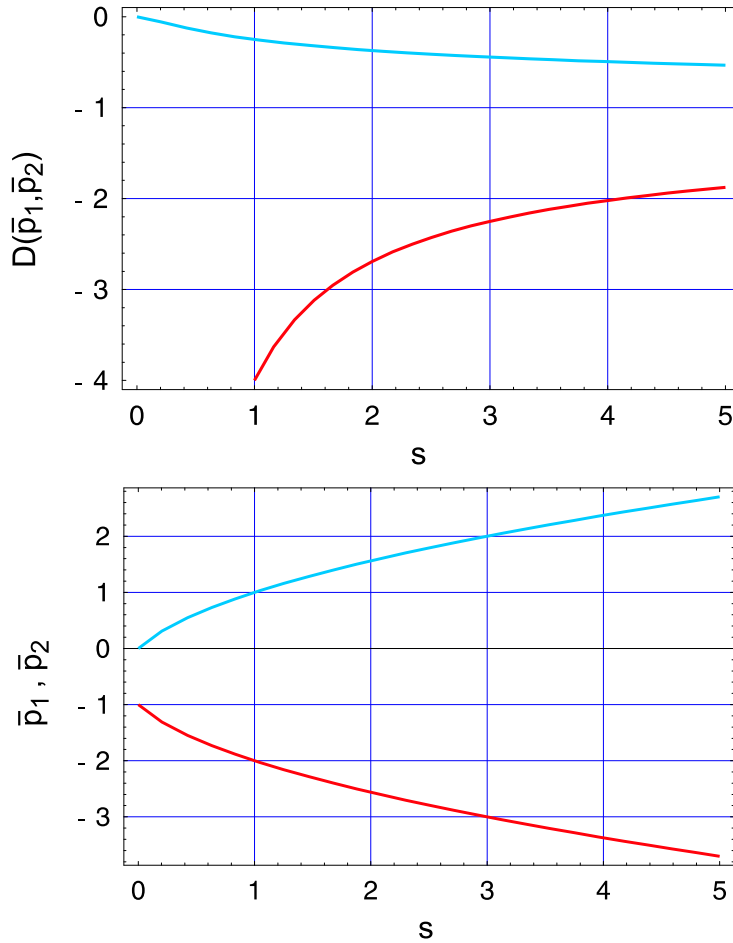
Figure 6: Position and stability of the two fixed points in the two-gene non-cooperative repression-repression system. As in the activation-activation case the regulatory determinant is non-positive, $D \leq 0$. The topmost plot shows $D(\bar{p}_1, \bar{p}_2)$ as a function of the auxiliary variable s for both fixed points. The fixed point $\bar{P}_1$ lies in the negative quadrant and is unstable, $D < -1$. The fixed point $\bar{P}_2$ is always situated in the physical protein space, the positive quadrant, and it is asymptotically stable since $0 \geq D \geq -1$ is fulfilled. Choice of parameters: $k_1^Q = k_2^Q = 2 \cdot s$, $K_1 = K_2 = 1$, and $k_1^P = k_2^P = d_1^Q = d_2^Q = d_1^P = d_2^P = 1$. Color code see 'Notation'.

Activation with leaky transcription. The effect of leaky transcription is illustrated in figures 7 and 8. For $\gamma_i > 0$ $(i = 1, 2)$ the fixed point at the origin is shifted either into the negative or into the positive quadrant such that exactly one fixed point is in each quadrant. The fixed point in physical protein space is always asymptotically stable, the one outside physical space is unstable. The scenario shown in figure 7 starts out from the position of the transcritical bifurcation in the limit $\gamma \to 0$. Accordingly, two states fulfilling the criteria mentioned above emerge at $\gamma > 0$, and the unstable state appears in the negative quadrant, $\bar{P}_1 = (\bar{p}_1^{(1)} < 0, \bar{p}_2^{(1)} < 0)$ and the stable fixed point is always inside the positive quadrant, $\bar{P}_2 = (\bar{p}_1^{(2)} > 0, \bar{p}_2^{(2)} > 0)$.

The plots in figure 8 illustrate the influence of weak basal transcription on the activation-activation regulatory system around the transcritical bifurcation point of the unperturbed system. An auxiliary variable is defined by
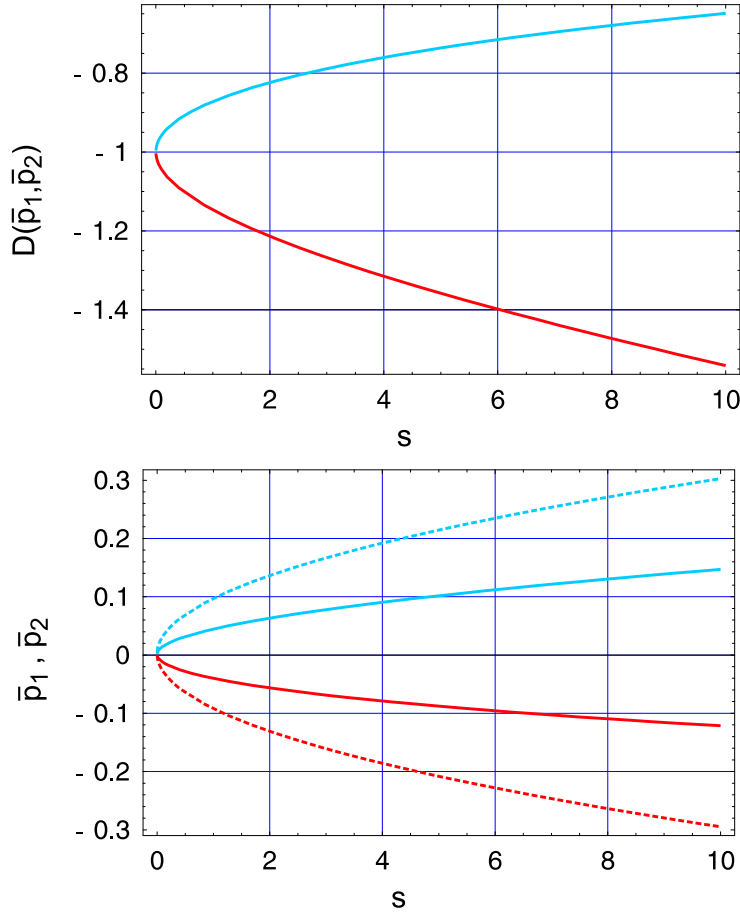
Figure 7: Position and stability of the two fixed points in the two-gene non-cooperative activation-activation system with leaky transcription: γ-dependence. Leaky transcription is introduced into the system exactly at the transcritical bifurcation point. The upper plot shows $D(\bar{p}_1, \bar{p}_2)$ for both fixed points as a function of an auxiliary variable s, which measures the extent of basal transcription, $\gamma_1 = \gamma_2 = 0.001 \cdot s$. The lower plot presents the positions of the two fixed points. For $s > 0$ the fixed point $\bar{P}_1$ lies in the negative quadrant and is unstable, $D < -1$. The fixed point $\bar{P}_2$ is always situated in the physical protein space, the positive quadrant, and it is asymptotically stable since $0 \geq D \geq -1$ is fulfilled. Choice of parameters: $k_1^Q = k_2^Q = 1$, $K_1 = 0.892857$, $K_2 = 4.464286$, $k_1^P = k_2^P = 1$, $d_1^Q = d_2^Q = 2$, and $d_1^P = d_2^P = 1$. Color code see 'Notation'.

$K_1 = 0.5/s$ and $K_2 = 2.5/s$ (The other parameter values are given in the caption of figure 8) and transcritical bifurcation is observe the at $s = 0.56$ ($\gamma_1 = \gamma_2 = 0$). Small gamma values gives rise to *avoided crossing*: At some distance from the virtual crossing point the two states are very close to those of the pure activation system and the continuation of these states at the other side of the virtual bifurcation point is readily recognized. The splitting for increasing $\gamma \geq 0$ at exactly this point was shown in the previous figure 7.

4.2 The cooperative binding case

For integer Hill coefficients $n \geq 2$ the binding curves have sigmoidal shape, the dynamics of the systems becomes richer and multiple steady states or
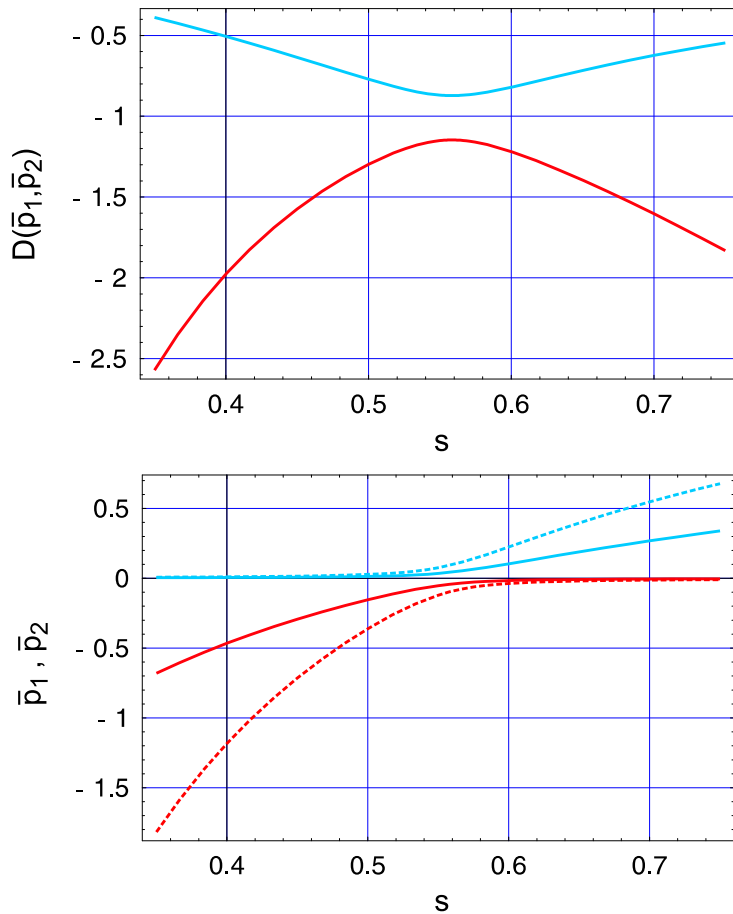
23

Figure 8: Position and stability of the two fixed points in the two-gene non-cooperative activation-activation system with leaky transcription: K-**dependence.** In contrast to figure 7 basal transcription occurs at a constant rate $\gamma_1 = \gamma_2 = 0.001$ as a function of the equilibrium parameters, $K_1 = 0.5/s$ and $K_2 = 2.5/s$. The upper plot shows $D(\bar{p}_1, \bar{p}_2)$ for both fixed points as a function of an auxiliary variable s in the neighborhood of the transcritical bifurcation at $s = 0.56$ for $\gamma_1 = \gamma_2 = 0$. The lower plot presents the positions of both points in the range of s. For $s > 0$ the fixed point $\bar{P}_1$ lies in the negative quadrant and is unstable, $D < -1$. The fixed point $\bar{P}_2$ is always situated in the physical protein space, the positive quadrant, and it is asymptotically stable since $0 \geq D \geq -1$ is fulfilled. Choice of other parameters: $k_1^Q = k_2^Q = 1$, $k_1^P = k_2^P = 1$, $d_1^Q = d_2^Q = 2$, and $d_1^P = d_2^P = 1$. Color code see 'Notation'.

oscillatory behavior emerge. As mentioned already in section 3.1 the polynomials for the computation of the positions of fixed points have an odd or even number of real solution for even or odd Hill coefficients n. Accordingly we find two or four solutions for $n = 1$ and $n = 3$, and one or three solutions for $n = 2$ and $n = 4$, respectively. Despite the high degrees of the polynomials in $\bar{p}_1$ or $\bar{p}_2$ $(n^2 + 1)$ we did not detect more stationary states up to $n = 4$. Although our searches of the high-dimensional parameter spaces were not exhaustive, it is unlikely that fixed points remained unnoticed. The rather small number of distinct states causes the dynamic patterns of the cooperative systems with different $n \geq 2$ to be qualitatively similar, with the only exception being activation-repression with $n = 2$, and therefore we shall group them only according to activation, repression, and basal transcription.
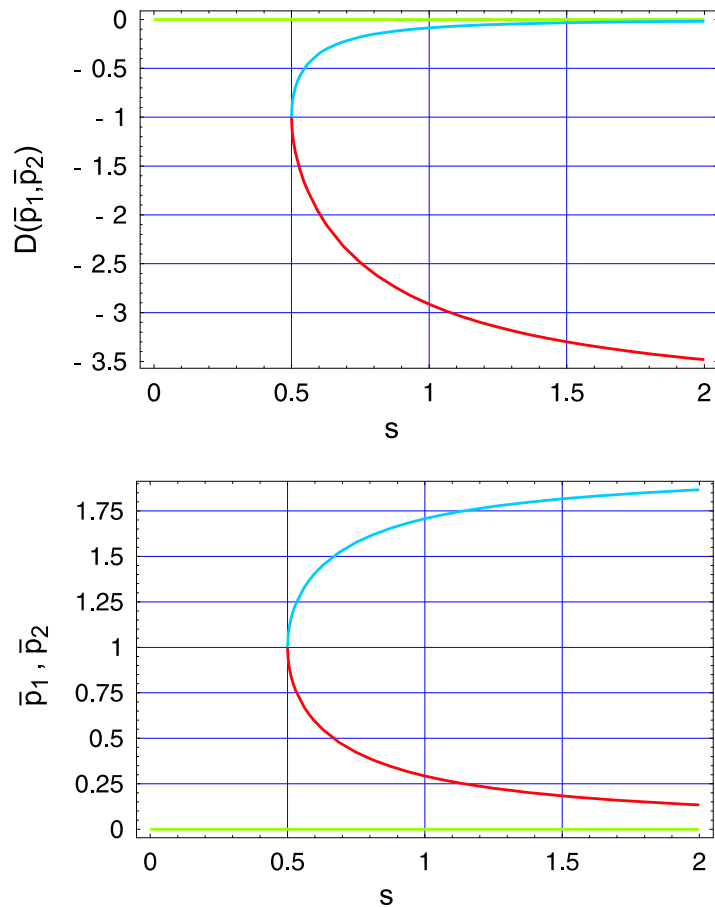
Figure 9: Position and stability of the fixed points in the two-gene cooperative activation-activation system with Hill coefficient $n = 2$. The properties of the system are studied as a function of the auxiliary variable s, which defines the binding constants: $K_1 = k_2 = 0.5/s$. The systems shows a saddle-node bifurcation at $s = 0.5$. Choice of the other parameters: $k_1^Q = k_2^Q = 2$, $k_1^P = k_2^P = d_1^Q = d_2^Q = d_1^P = d_2^P = 1$. Color code see 'Notation'.

Activation-activation. For $n = 2$ the expansion of equation (16) yields a polynomial of degree five. Numerical solution yields one or three solutions in the positive quadrant including the origin which correspond to one or three steady states. The origin represents one fixed point, $\bar{P}_1 = (0,0)$ that, in contrast to the non-cooperative system is always stable.[8] Searching parameter space in the direction of increasing transcription rate parameters, $(k_1^Q = \chi_1 \cdot s, k_2^Q = \chi_2 \cdot s)$, and/or decreasing dissociation constants of regulatory complexes, $(K_1 = \lambda_1/s, K_2 = \lambda_2/s)$, yields a saddle-node bifurcation when the condition $D = D_{\text{oneD}}$ of equation (23) is fulfilled (figure 9). At this point, separating the unregulated regime with the origin being the only stable state from the regulated regime, two new fixed points appear and branch off, thereby fulfilling the conditions $D < D_{\text{oneD}}$ and $D > D_{\text{oneD}}$, respectively. The former fixed point is unstable – at least for some range in parameter space – whereas the latter fixed point is asymptotically stable since D can only adopt negative signs (For examples with no sign restriction on D see below in the

---

[8]This result follows straightforwardly from a computation of the derivatives in the Jacobian, which yields $D = 0$ at the origin for all Hill coefficients $n > 1$.

Table 2: Dependence of the bifurcation point on the Hill coefficient n.
The value of the auxiliary variable s at the bifurcation point that separates the unregulated regime and the regulated regime is compared for different cooperative regulation modes and Hill coefficients $n = 2, 3, 4$. In order to allow for comparison equivalent paths through parameter space were chosen for all three classes of systems.

System	Bifurcation type	Parameter variation	Variable s at bifurcation		
			$n = 2$	$n = 3$	$n = 4$
act-act[a]	saddle-node	$K_1 = K_2 = 0.5/s$ [b]	0.5	0.422	0.296
act-rep	Hopf	$K_1 = K_2 = 0.5/s$ [b]	–	2.772	0.5
rep-rep	pitchfork[c]	$K_1 = K_2 = 0.5/s$ [b]	0.5	0.106	0.033

[a] In case of **act-act** other paths through parameter space lead to small or almost vanishing dependencies of the bifurcation value of s on the Hill coefficient n, for example we found $s = 0.79, 0.81, 0.78$ for $n = 2, 3, 4$, $k_1^Q = k_2^Q = 2 \cdot s$, $K_1 = K_2 = 0.5/s$ and $s = 1, 0.96, 0.90$ for $k_1^Q = k_2^Q = 2 \cdot s$, $K_1 = K_2 = 1/s$, respectively (All other parameters being one).

[b] The other parameter values were: $k_1^Q = k_2^Q = 2$ and $k_1^P = k_2^P = d_1^Q = d_2^Q = d_1^P = d_2^P = 1$.

[c] The pitchfork bifurcation becomes a saddle-node bifurcation, when the symmetry consisting of identical parameters for gene 1 and gene 2 is broken (See figure 13).

paragraph dealing with intermediate cases). Raising the Hill coefficient from $n = 2$ to $n = 3$ and to $n = 4$ has rather little effect on the position of the bifurcation point. As shown in table 2 we find somewhat smaller values of s at the bifurcation point for the higher Hill coefficients, but the changes are much smaller than for the activation-repression and the repression-repression system. In addition this weak dependence is replaced by even weaker or no dependence on n when the implementation of the auxiliary variable s is changed.

Activation-repression. The activation-repression with $n = 2$ is characterized by a nonnegative regulatory determinant ($D \geq 0$), but as discussed in section 3.2 the maximal value of D is insufficient for a Hopf bifurcation. The system exhibits only one stable fixed point and no undamped oscillations can occur. In other words, the **act-rep** systems with $n = 1$ and $n = 2$ show only an 'unregulated regime'.

For $n \geq 3$, however, a Hopf bifurcation is predicted and a limit cycle can be observed for sufficiently strong binding (figures 10 and 11). Systems of this class exhibit periodically changing gene activities. Oscillation in regulatory systems can be used as a pacemaker inducing periodicity into metabolism as it occurs, for example, in circadian and other rhythms. The qualitative picture of the bifurcation diagram is essentially the same for Hill coefficients $n = 4$ and larger. Along equivalent trajectories leading from the unregulated to the regulated regime the Hopf bifurcation occurs at substantially smaller s-values than for $n = 3$. In other words, the regulated domain in parameter space – here the domain that contains an unstable fixed point and a limit
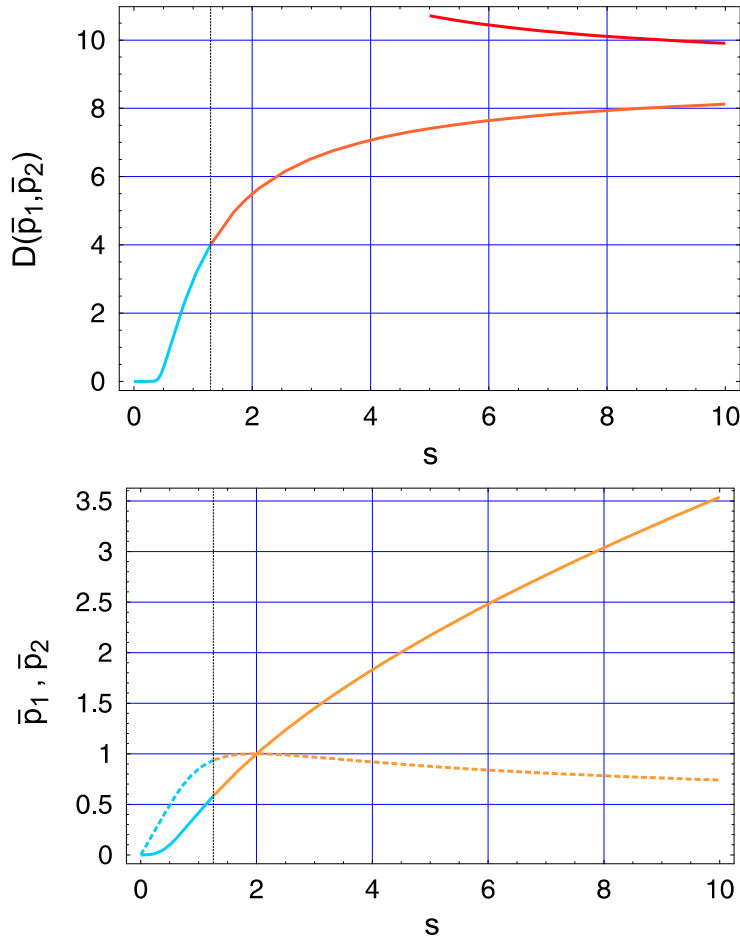
Figure 10: Position and stability of the fixed points in the two-gene cooperative activation-repression system with Hill coefficient $n = 3$. The regulatory determinant is non-negative, $D \geq 0$. The properties of the dynamical system, shown here as functions of the auxiliary variable s, $k_1^Q = k_2^Q = 2s$ and $K_1 = K_2 = 0.5/s$, change at the Hopf bifurcation observed at $s = 1.2903$ (vertical line in the plots): The central fixed point becomes unstable and a limit cycle appears (See figure 11). Choice of other parameters: $k_1^P = k_2^P = d_1^Q = d_2^Q = d_1^P = d_2^P = 1$. Color code see 'Notation'.

cycle – becomes larger with increasing cooperativity as expressed by higher Hill coefficients.

Repression-repression. The cooperative repression-repression system is the prototype of a genetic switch. At low affinities the system sustains one asymptotically stable stationary state. In the regulated regime it shows bistability consisting of two asymptotically stable states that can be characterized as $\mathbf{G}_1$ active and $\mathbf{G}_2$ silenced and vice versa, $\mathbf{G}_2$ active and $\mathbf{G}_1$ unregulated. The two states are separated by a saddle point (figures 12 and 13). For symmetric choices of parameters, implying that all parameters for $\mathbf{G}_1$ have values identical to those of the corresponding parameters for $\mathbf{G}_2$, a pitchfork bifurcation separates the unregulated regime from the regulated regime. Introducing asymmetry through different values for k_1^Q and k_2^Q and/or K_1 and K_2, respectively, removes the degeneracy leading to the pitchfork and a sad-
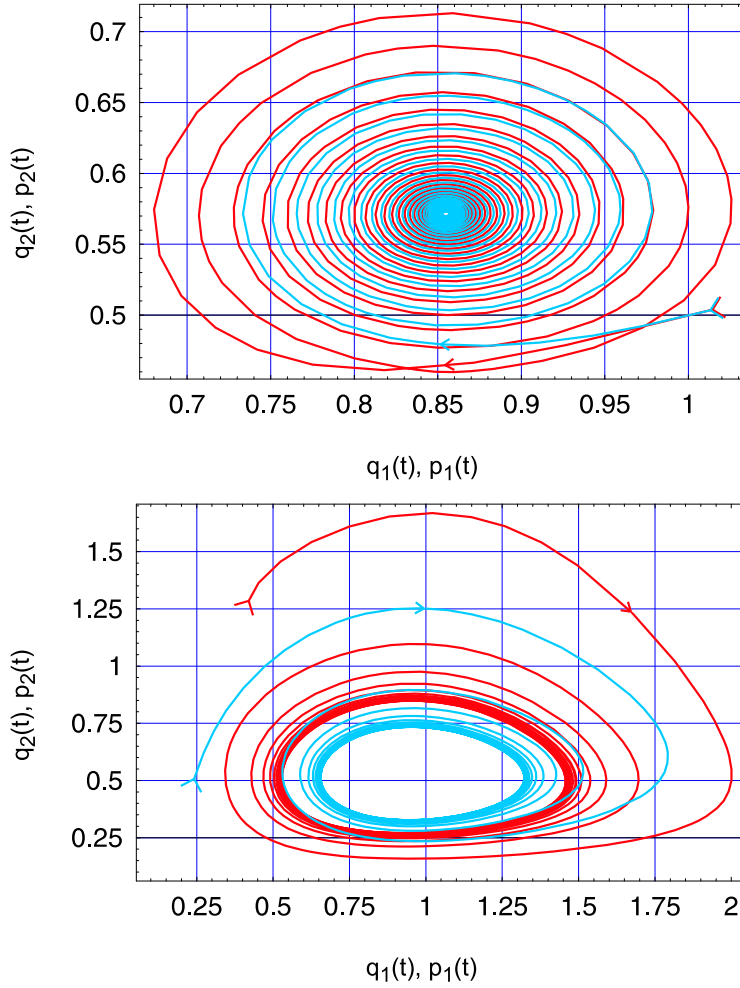
Figure 11: Stable fixed point and limit cycle in the two-gene cooperative activation-repression system with Hill coefficient $n = 3$. The two plots show trajectories of the system before and after the Hopf bifurcation that occurs at $D(s) = 4$ with $s_{\text{Hopf}} = 2.17$ in the system with $k_1^Q = k_2^Q = 1 \cdot s$ and $K_1 = K_2 = 0.5/s$ and $k_1^P = k_2^P = d_1^Q = d_2^Q = d_1^P = d_2^P = 1$. The upper plot shows a trajectory for $s = 2$ ($D(2) = 3.6804$) with a stable fixed point and the trajectories spiralling inwards, the lower plot was recorded for $s = 2.5$ ($D(2.5) = 4.5265$) where the fixed point is unstable and a stable limit cycle is observed. The trajectories spiral form outside towards the limit cycle. For initial conditions near the unstable fixed point the limit cycle is approached through spiralling outwards (not shown). Color code: The projection of the trajectory onto the mRNA concentration subspace, $\big(q_1(t), q_2(t)\big)$, is shown in red and the alternative projection onto the protein subspace, $\big(p_1(t), p_2(t)\big)$ is plotted in blue.

dle node bifurcation remains. As illustrated nicely by the parametric plot in the middle of figure 13 the stable fixed point of the unregulated regime is attracted towards the (no more existing) point of the pitchfork. Such a phenomenon is often called the influence of a 'ghost' on bifurcation lines or trajectories. Considering identical paths through parameter space the position of the pitchfork bifurcation is shifted towards smaller values of the auxiliary parameter s in the series $n = 2, 3, 4$ (table 2).
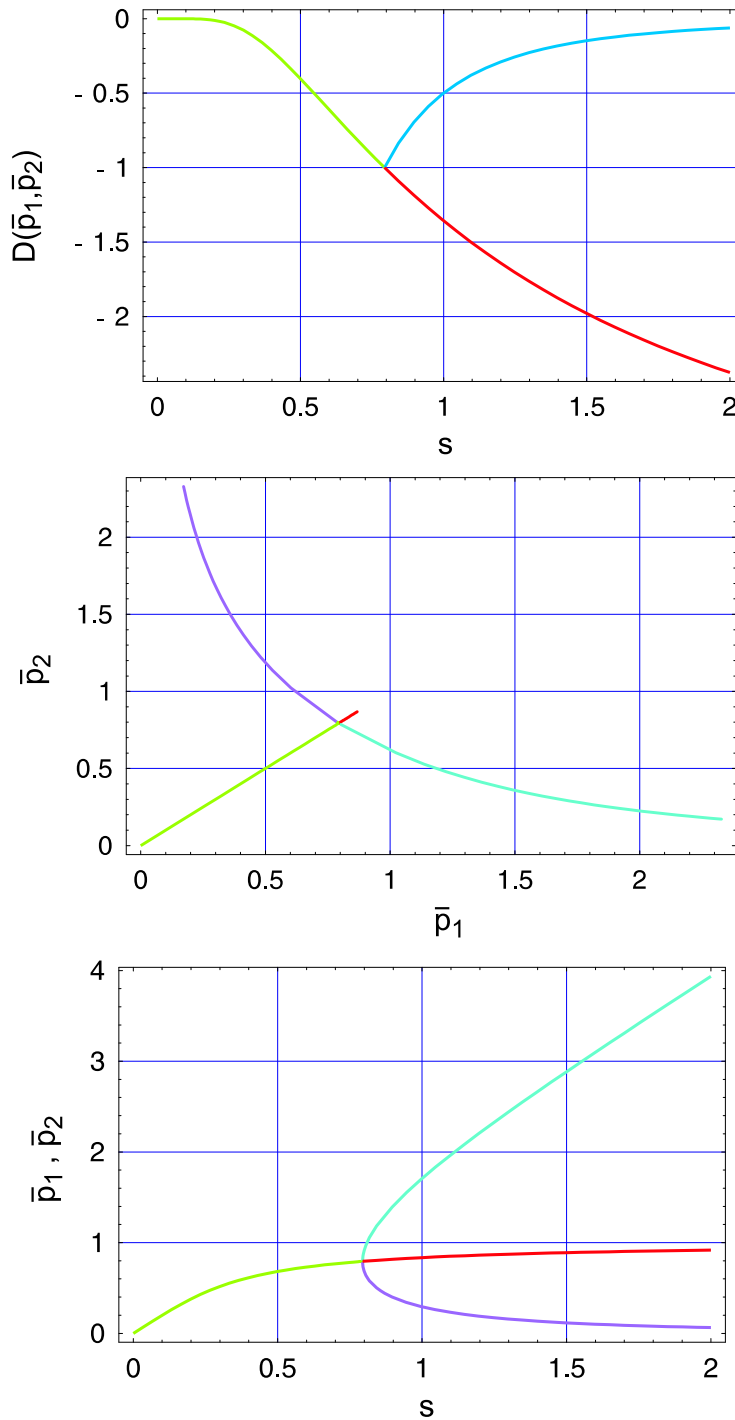
Figure 12: Position and stability of the two fixed points in the two-gene cooperative repression-repression system with $n = 2$ and symmetric choice of parameters. In the symmetric case the one dimensional bifurcation is a pitchfork at the value $s = 0.7937$ for the following choice of parameters: $k_1^Q = k_2^Q = 2 \cdot s$, $K_1 = K_2 = 0.5/s$, and $k_1^P = k_2^P = d_1^Q = d_2^Q = d_1^P = d_2^P = 1$. The topmost plot shows the dependence of the regulatory determinants on s (By symmetry reasons the violet and the turquoise curve are on top of each other and only the latter can be seen). in the middle we present a parametric plot of the positions of all fixed points, $(\bar{p}_1(s), \bar{p}_2(s))$, and the picture at the bottom shows these positions as function of s. Color code see 'Notation'.
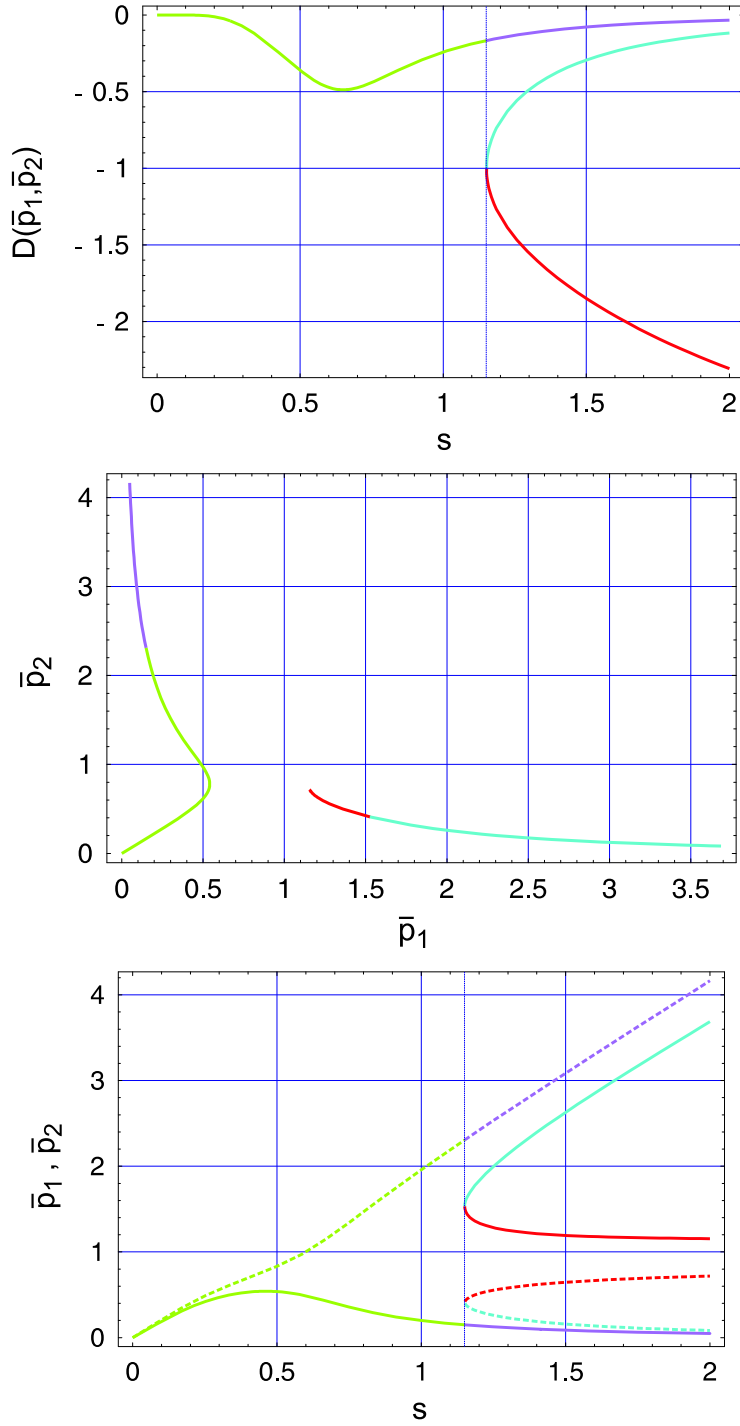
Figure 13: Position and stability of the two fixed points in the two-gene cooperative repression-repression system with $n = 2$ and asymmetric choice of parameters. In the asymmetric case the pitchfork bifurcation is replaced by a saddle node bifurcation that occurs here at $s = 1.1515$ for the parameter choice: $k_1^Q = 1.9 \cdot s$, $k_2^Q = 2 \cdot s$, $K_1 = 0.55/s$, $K_2 = 0.45/s$, and $k_1^P = k_2^P = d_1^Q = d_2^Q = d_1^P = d_2^P = 1$. The topmost plot shows the dependence of the regulatory determinants on s, in the middle we present a parametric plot of the positions of all fixed points, $(\bar{p}_1(s), \bar{p}_2(s))$, and the picture at the bottom shows the coordinates of the fixed points as functions of s. Color code see 'Notation'.
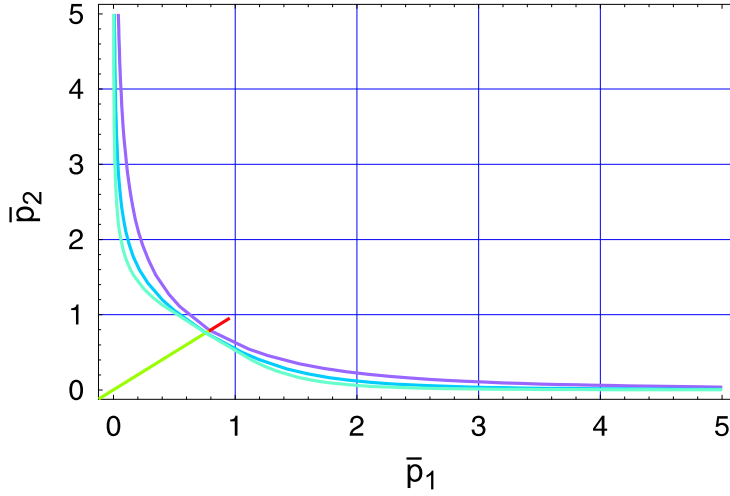
Figure 14: Position of fixed points in the two-gene cooperative repression-repression system. The parametric plot shows a superposition of the pitchfork diagrams for the Hill coefficients $n = 2, 3$, and 4 with the varied parameters $k_1^Q = k_2^Q = 2 \cdot s$ and $K_1 = K_2 = 0.5/s$ defining the path through parameter space. Choice of the other parameters: $k_1^P = k_2^P = d_1^Q = d_2^Q = d_1^P = d_2^P = 1$. Color code see 'Notation'.

Genetic switches with different Hill coefficients. The regulatory properties of repression-repression systems are of primary interest in computations of genabolic networks. As said above, the value of s at the pitchfork or saddle-node bifurcation decreases substantially for increasing Hill coefficients (table 2). Two more properties are highly relevant in the context of regulation: (i) The 'pitchforks' in parametric plots for different Hill coefficients are surprising similar (figure 14) and (ii) the regulatory selectivity increases strongly in the sequence $n = 2$, 3, and 4 (table 3).

The superposition of the three pitchfork diagrams in figure 14 reveals astonishing agreements of the plots for three different Hill coefficients ($n = 2, 3, 4$). This general behavior is changed slightly only when different paths through parameter space are chosen as long as $k_1^Q = \chi_1 \cdot s$ and $k_2^Q = \chi_2 \cdot s$ is applied for the kinetic parameters. Constant values of K_1 and K_2, for example, have little influence on the diagram. If the dissociation constants, however, are varied, for example $K_1 = \lambda_1/s$ and $K_2 = \lambda_2/s$, and two kinetic parameters are chosen to be constant, the bifurcation diagram changes shape substantially. The differences in the plots are explained readily by inspection of the limits derived for the paths through parameter space. As an example we present the limits of the fixed points for the two cases mentioned above (See also table 1):

$$\vartheta_1 = \delta_1 \cdot s, \vartheta_2 = \delta_2 \cdot s, K_1, K_2 : \quad \lim_{s \to 0} \bar{P}_1 = (0,0), \lim_{s \to \infty} \bar{P}_1 = (\infty, \infty)$$

$$\lim_{s \to \infty} \bar{P}_2 = (\infty, 0), \quad \lim_{s \to \infty} \bar{P}_3 = (0, \infty)$$

$$\vartheta_1, \vartheta_2, K_1 = \lambda_1/s, K_2 = \lambda_2/s : \quad \lim_{s \to 0} \bar{P}_1 = (\vartheta_1, \vartheta_2), \lim_{s \to \infty} \bar{P}_1 = (0,0)$$

$$\lim_{s \to \infty} \bar{P}_2 = (\vartheta_1, 0), \quad \lim_{s \to \infty} \bar{P}_3 = (0, \vartheta_2) .$$

Simultaneous variation of the ϑ-parameters and the equilibrium constants

Table 3: Position of the bifurcation point in repression-repression systems and switching efficiency for different Hill coefficients $n = 2, 3, 4$. The values in the table are sampled on equivalent paths through parameter space with the following parameter values: $k_1^Q = k_2^Q = 2$, $K_1 = K_2 = 1/s$ and $k_1^P = k_2^P = d_1^Q = d_2^Q = d_1^P = d_2^P = 1$. Because of symmetry the bifurcation is of pitchfork type.

n	Variable s at bifurcation	Position $\bar{p}_1 = \bar{p}_2$	Silencing efficiency[a] $s = 1.5$	$s = 2.5$	$s = 4.0$
2	1	1	(1.577,0.423)	(1.775,0.225)	(1.866,0.134)
3	0.2109	1.333	(1.989,0.156)	(1.996,0.096)	(1.998,0.061)
4	0.0685	1.500	(2.000,0.080)	(2.000,0.049)	(2.000,0.031)

[a] The values in parentheses represent the stationary concentrations of regulators proteins, $(\bar{p}_1, \bar{p}_2)$, at the fixed point $\bar{P}_1$ for the given value of the auxiliary variable s.

K results in the same behavior as variation of the former parameters alone. Clearly, only patterns with the same limits are comparable and in the current example we chose the former case, variation of kinetic parameters with or without variation of dissociation constants.

In table 3 the efficiency of genetic switches is compared for different Hill coefficients. The numbers illustrate the effect of higher order cooperativity: The higher the value of n, the larger is the selective power of the switch. At $s = 4$, for example, we find the mole fractions[9] $\bar{x}_2 = 0.067$, 0.030, and 0.015 for the protein of the silenced gene for the Hill coefficients $n = 2, 3$, and 4, respectively. Since the pitchfork diagrams are not very different for the three cases the efficiency in silencing is caused by the different values of s at comparable points. An illustration for this argument is given by the bifurcation point itself which occurs at $s = 1$, 0.211, and 0.069 for $n = 2, 3$, and 4, respectively.

Summarizing cooperative repression-repression systems we recognize their importance as genetic switches. Hill coefficients higher than $n = 2$ have two properties that are relevant for regulation: (i) The regulated regime comprises a larger domain in parameter space, and (ii) the selectivity of the regulatory function increases with increasing n.

Activation with basal transcription. The cooperative case of activation (n=2) with leaky transcription provides an illustrative example of a system with two saddle-node bifurcations, $(s_{\text{oneD}})_1$ and $(s_{\text{oneD}})_2$, which gives rise to hysteresis. Figure 15 presents the fixed points as functions of spontaneous transcription rate parameter γ. In this figure the parameters were chosen such that the system has only one fixed point at $\lim \gamma \to 0$, the stable origin. With increasing values of γ the system undergoes a saddle-node bifurcation that leads to the regulated regime with two asymptotically stable fixed points, one at high and one at low stationary protein concentrations,

---

[9]The mole fraction is defined by $\bar{x}_i = \bar{p}_i/(\bar{p}_1 + \bar{p}_2)$ for $i = 1, 2$.
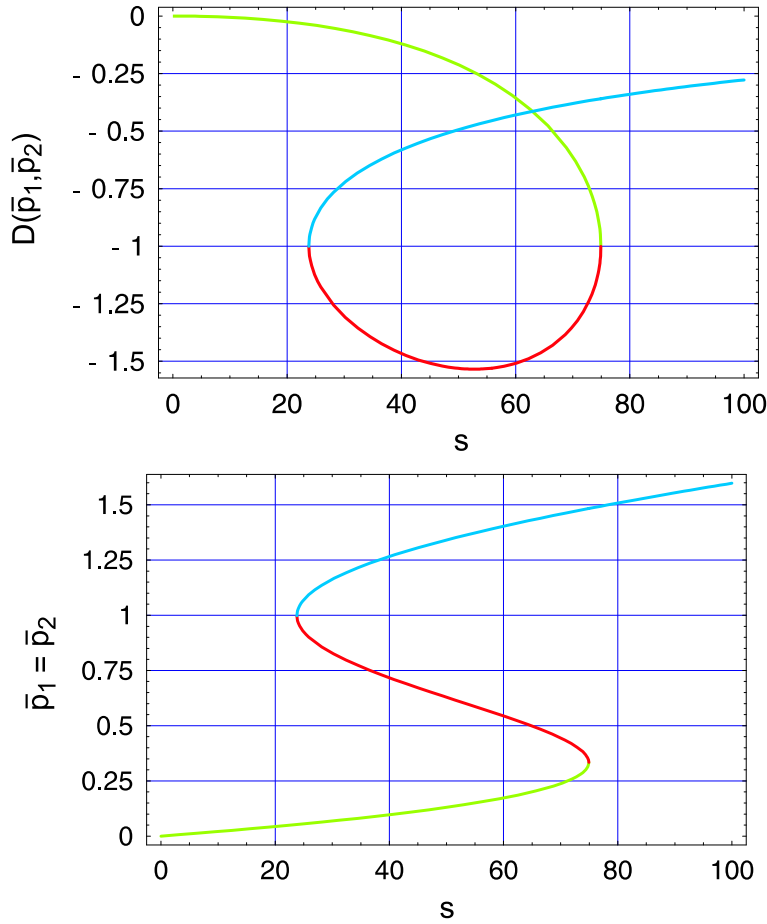
Figure 15: Position and stability of the two fixed points in the two-gene cooperative activation-activation system with leaky transcription.
The influence of basal transcription activity on the bifurcation behavior of the act-act system with $n = 2$ is illustrated by variation of γ as in figure 7 according to $\gamma_1 = \gamma_2 = 0.001 \cdot s$. The system passes through two saddle node bifurcations at $s = 23.81$ and $s = 74.92$, and it shows hysteresis. Choice of parameters: $k_1^Q = k_2^Q = 2$, $K_1 = K_2 = 1.1$, and $k_1^P = k_2^P = d_1^Q = d_2^Q = d_1^P = d_2^P = 1$. Color code see 'Notation'.

separated by a saddle. Further increase in γ, however, leads to a second saddle-node bifurcation that annihilates the stable state originating from the origin together with the unstable saddle. The state that eventually remains is the high activity state (both genes active) which originates in the first saddle-node bifurcation.

As shown in figure 15 the sequence of bifurcations gives rise to hysteresis in the range between the two bifurcation points, $(s_{\mathsf{oneD}})_1 < s < (s_{\mathsf{oneD}})_2$. Coming from high values of γ the system stays in the high protein concentration branch (as long as it is not shifted to the low concentration state by fluctuations), the low protein concentration branch, on the other hand, is reached from s values below $(s_{\mathsf{oneD}})_1$.

The existence of a single stable state at high values of s and with high protein concentrations is easy to predict from the reaction kinetics: With increasing γ-values spontaneous transcription will, at some point, dominate and then only the non-regulated stationary state exists. This situation, how-

ever, is unlikely to occur in realistic biological systems, because unregulated transcription is common at very low levels only. The second saddle-node bifurcation – although not natural – could well be of interest for the design of artificial regulatory systems since it allows for up and down regulation of gene activity in an intermediate range.

Influence of basal transcription on bifurcation patterns. The influence of basal transcription on all three classes of regulatory systems (**act-act**, **act-rep**, and **rep-rep**) is compared in figure 16. For simplicity the diagrams show only the symmetric cases, $\gamma_1 = \gamma_2 = \gamma$ and $\vartheta_1 = \vartheta_2 = \vartheta$, and the systems with the lowest values of the Hill coefficient at which the characteristic bifurcation pattern appears ($n = 2$ for **act-act** and **rep-rep**, and $n = 3$ for **act-rep**). All three systems have in common that the bifurcations vanish at sufficiently large values of $\gamma > \gamma_{\mathrm{crit}}$ and then the systems sustain only one stable state. Below γ_{crit} we find the specific bifurcation pattern for the systems in a certain range $\vartheta_{\mathrm{crit}}^{(1)} < \vartheta < \vartheta_{\mathrm{crit}}^{(2)}$: The bifurcation at low values of ϑ is compensated by an inverse bifurcation of the same class at higher ϑ-values. For all systems the inverse bifurcation point approaches infinity for vanishing basal transcription: $\lim_{\gamma \to 0} \vartheta_{\mathrm{crit}}^{(2)} = +\infty$. There is, however, one characteristic difference between the three bifurcation diagrams: The lower bifurcation line has a negative slope in the **act-act** system but a positive slope in the two other classes, **act-rep** and **rep-rep**. This implies that for increasing basal transcription, $\gamma < \gamma_{\mathrm{crit}}$ the saddle-node bifurcation occurs at lower values of ϑ, whereas increasing basal activity drives the first bifurcation to higher ϑ-values in the other two classes of systems.

Two examples of intermediate regulation. In order to illustrate the bifurcation pattern with respect to regulatory determinants D that can change sign we consider two examples of regulation by intermediate complexes: (i) a combination of activation and intermediate regulation and (ii) a combination of repression and intermediate regulation. Both cases have a Hill coefficient $n = 4$. The four complexes formed by successive binding are show together with the various forms of potential transcriptional regulation in figure 17. The four dissociation constants are multiplied to yield the following combinations:

$$\kappa_{11} = K_1^{(1)} \cdot K_2^{(1)} \cdot K_3^{(1)} \cdot K_4^{(1)}, \ \ \kappa_{12} = K_2^{(1)} \cdot K_3^{(1)} \cdot K_4^{(1)}, \ \ \kappa_{13} = K_3^{(1)} \cdot K_4^{(1)}, \ \ \kappa_{14} = K_4^{(1)}$$

$$\kappa_{21} = K_1^{(2)} \cdot K_2^{(2)} \cdot K_3^{(2)} \cdot K_4^{(2)}, \ \ \kappa_{22} = K_2^{(2)} \cdot K_3^{(2)} \cdot K_4^{(2)}, \ \ \kappa_{23} = K_3^{(2)} \cdot K_4^{(2)}, \ \ \kappa_{24} = K_4^{(2)}.$$

As mentioned in section 2.1 the equilibrium parameters used here are macroscopic dissociation constants.

In the first system the saturated complex $\mathbf{H}_2^{(4)} \left(F_1(\bar{p}_2) \right)$ and the 'intermediate 2' $\mathbf{H}_2^{(2)} \left(F_2(\bar{p}_1) \right)$ initiate transcription and the binding functions are of the form

$$F_1(\bar{p}_2) = \frac{\bar{p}_2^4}{\kappa_{21} + \kappa_{22}\bar{p}_2 + \kappa_{23}\bar{p}_2^2 + \kappa_{24}\bar{p}_2^3 + \bar{p}_2^4} \quad \text{and}$$

$$F_2(\bar{p}_1) = \frac{\kappa_{13}\,\bar{p}_1^2}{\kappa_{11} + \kappa_{12}\bar{p}_2 + \kappa_{13}\bar{p}_1^2 + \kappa_{14}\bar{p}_1^3 + \bar{p}_1^4} \ .$$
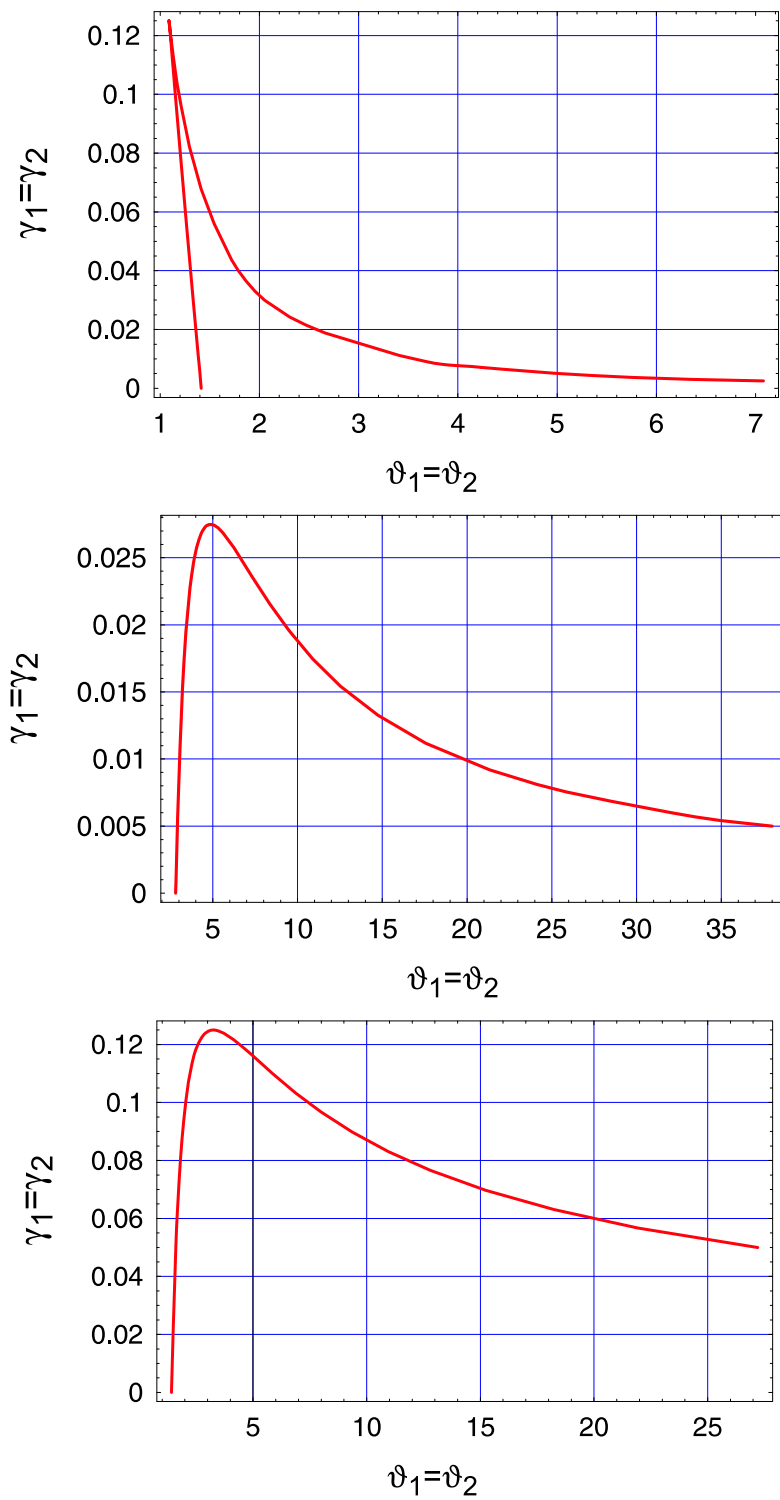
Figure 16: The influence of basal transcription on the bifurcation patterns of gene regulation. The topmost plot presents the positions of the saddle-node bifurcations of the **act-act** system with Hill coefficient $n = 2$ in the (ϑ, γ)-plane. In the area to the right of the first and below the second curve we observe three stationary states, elsewhere one stable stationary state. The plot in the middle refers to the **act-rep** system with Hill coefficient $n = 3$: Oscillations occur below the bifurcation curve. The plot at the bottom shows the analogous curve of the **rep-rep** system with Hill coefficient $n = 2$. Three steady states are observed between two (opposite) pitchfork bifurcations, i.e. in the area below the curve. Other parameters: $K_1 = K_2 = 0.5$, and $k_1^{\mathrm{Q}} = \vartheta_1 = k_2^{\mathrm{Q}} = \vartheta_2$, $k_1^{\mathrm{P}} = k_2^{\mathrm{P}} = d_1^{\mathrm{Q}} = d_2^{\mathrm{Q}} = d_1^{\mathrm{P}} = d_2^{\mathrm{P}} = 1$ for the middle plot.

$$4\,P_2 + G_1 \xrightarrow{\;k_1^Q \cdot F_1^{act}(p_2)\;} G_1 + P_1$$
Repression

$\kappa_2^{(1)} \big\updownarrow$

$$3\,P_2 + H_1^{(1)} \xrightarrow{\;k_1^Q \cdot F_1^{int1}(p_2)\;} H_1^{(1)} + P_1$$
Intermediate 1

$\kappa_2^{(2)} \big\updownarrow$

$$2\,P_2 + H_1^{(2)} \xrightarrow{\;k_1^Q \cdot F_1^{int2}(p_2)\;} H_1^{(2)} + P_1$$
Intermediate 2

$\kappa_2^{(3)} \big\updownarrow$

$$P_2 + H_1^{(3)} \xrightarrow{\;k_1^Q \cdot F_1^{int3}(p_2)\;} H_1^{(3)} + P_1$$
Intermediate 3

$\kappa_2^{(4)} \big\updownarrow$

$$H_1^{(4)} \xrightarrow{\;k_1^Q \cdot F_1^{rep}(p_2)\;} H_1^{(4)} + P_1$$
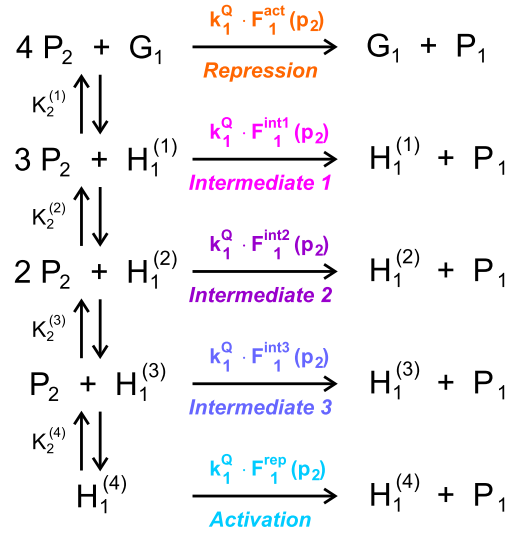*Activation*

Figure 17: Intermediate complexes as active forms in transcription.
A four step binding equilibrium of four monomers to a binding site in the gene regulatory region is shown as an example for the dynamics of regulation by means of active intermediate complexes. Three intermediate complexes, $\mathbf{H}_i^{(1)}$, $\mathbf{H}_i^{(2)}$, and $\mathbf{H}_i^{(3)}$ are potential candidates for transcription.

Computation of the regulatory determinant D is straightforward and yields

$$D(\bar{p}_1, \bar{p}_2) = -k_1^Q k_2^Q k_1^P k_2^P \cdot$$

$$\cdot \frac{\kappa_{13}\bar{p}_1\bar{p}_2^3(2\kappa_{11} + \kappa_{12}\bar{p}_1 - \kappa_{14}\bar{p}_1^3 - 2\bar{p}_1^4)(4\kappa_{21} + 3\kappa_{22}\bar{p}_2 + 2\kappa_{23}\bar{p}_2^2 + \kappa_{24}\bar{p}_2^3)}{(\kappa_{11} + \kappa_{12}\bar{p}_2 + \kappa_{13}\bar{p}_1^2 + \kappa_{14}\bar{p}_1^3 + \bar{p}_1^4)^2(\kappa_{21} + \kappa_{22}\bar{p}_2 + \kappa_{23}\bar{p}_2^2 + \kappa_{24}\bar{p}_2^3 + \bar{p}_2^4)^2} \cdot$$

In principle, D can adopt plus and minus signs and a Hopf bifurcation may occur in addition to the one dimensional bifurcation of **act-act** systems. The system sustains one or three stationary states. The state at the origin is always stable. Then it passes through two bifurcations as a function of the auxiliary variable s. The first of them is a saddle-node bifurcation at $s = s_{\mathsf{oneD}}$, which is found in all cooperative activation-activation systems and where two more states are formed. The new stable state moves outwards in the positive quadrant, i.e. to larger values of $\bar{p}_1$ and $\bar{p}_2$, and the unstable state moves inwards. As shown in figure 18 the system passes indeed a Hopf bifurcation at $s = s_{\mathsf{Hopf}}$ and a stable limit cycle is formed.

The second example of intermediate regulation combines repression $\big(F_1(\bar{p}_2)\big)$ and an active intermediate complex $\big(F_2(\bar{p}_1)\big)$. Here $\mathbf{G}_1$ and the 'intermediate 2' $\mathbf{H}_2^{(2)}$ are the active transcription forms. The two regulatory functions are given by

$$F_1(\bar{p}_2) = \frac{\kappa_{21}}{\kappa_{21} + \kappa_{22}\bar{p}_2 + \kappa_{23}\bar{p}_2^2 + \kappa_{24}\bar{p}_2^3 + \bar{p}_2^4} \quad \text{and}$$

$$F_2(\bar{p}_1) = \frac{\kappa_{13}\,\bar{p}_1^2}{\kappa_{11} + \kappa_{12}\bar{p}_2 + \kappa_{13}\bar{p}_1^2 + \kappa_{14}\bar{p}_1^3 + \bar{p}_1^4} \;.$$
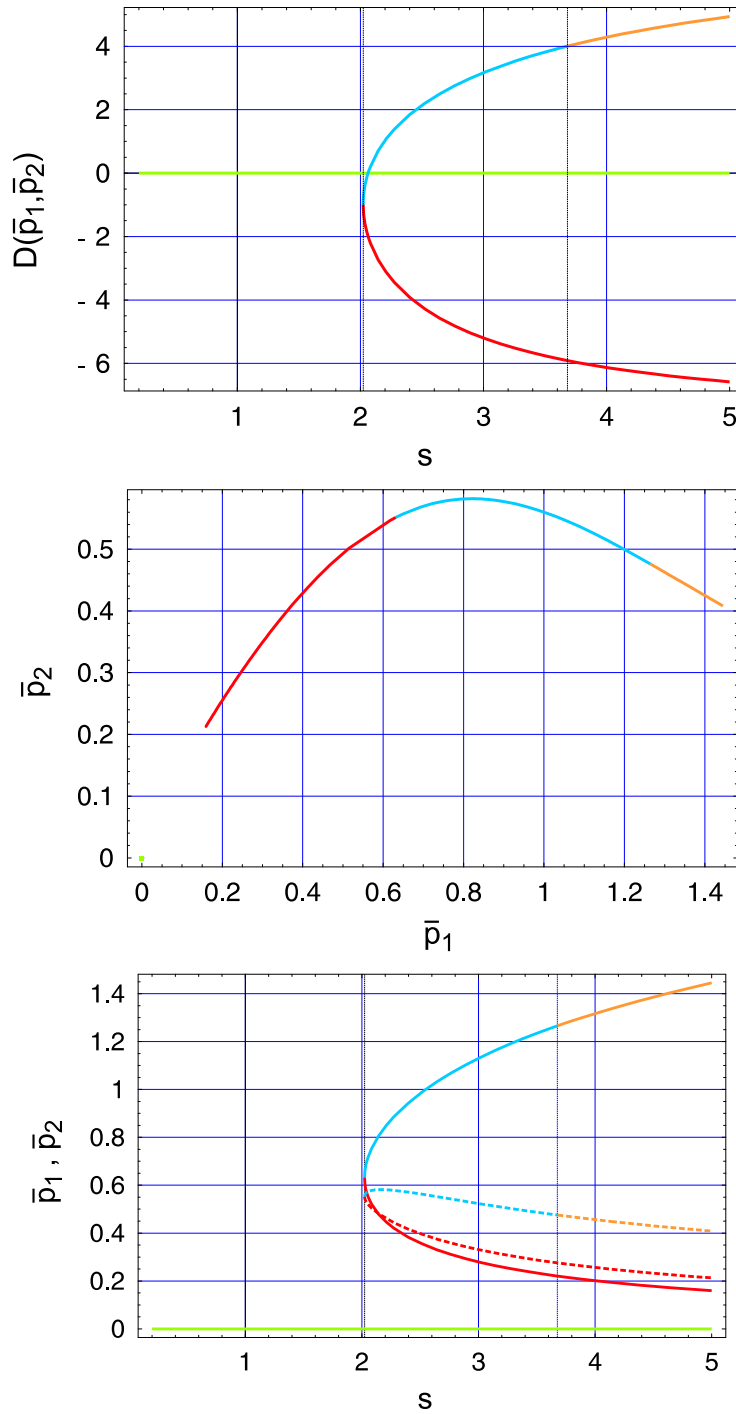
Figure 18: Position and stability of the fixed points in the two-gene cooperative system with intermediate activation and a Hill coefficient of $n = 4$**.** The active entities are $\mathbf{H}_1^{(4)}$ and $\mathbf{H}_2^{(2)}$. A saddle-node bifurcation $s = 2.023$ and a Hopf bifurcation $s = 3.671$ are observed. Choice of parameters: $k_1^Q = k_2^Q = 2 \cdot s$, $\kappa_{11} = \kappa_{12} = \ldots = \kappa_{24} = 0.5/s$, and $k_1^P = k_2^P = d_1^Q = d_2^Q = d_1^P = d_2^P = 1$. Color code see 'Notation'.
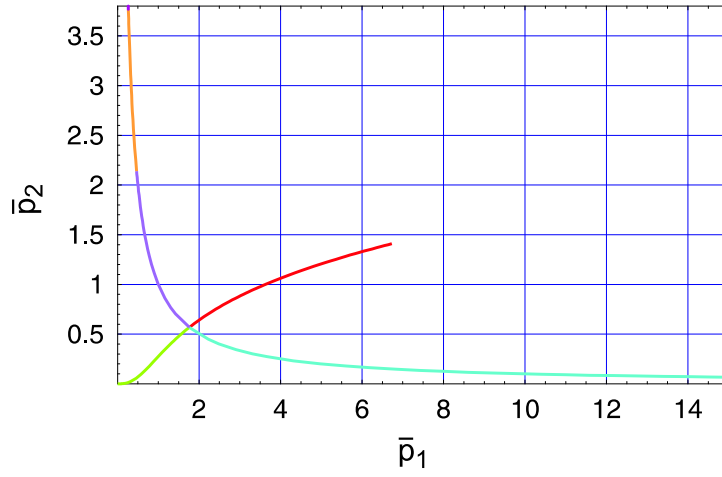
Figure 19: Position and stability of the two fixed points in the two-gene cooperative system with intermediate repression and Hill coefficient $n = 4$. The active entities are G_1 and $\mathsf{H}_2^{(2)}$. A pitchfork bifurcation bifurcation at $s = 3.834$ and a Hopf bifurcation at $s = 17.96$ are observed. Choice of parameters: $k_1^Q = k_2^Q = 1 \cdot s$, $\kappa_{11} = \kappa_{12} = \ldots = \kappa_{24} = 1$, and $k_1^P = k_2^P = d_1^Q = d_2^Q = d_1^P = d_2^P = 1$. Color code see 'Notation'.

Computation of the regulatory determinant D yields now

$$D(\bar{p}_1, \bar{p}_2) = k_1^Q k_2^Q k_1^P k_2^P \cdot$$

$$\cdot \frac{\kappa_{13}\kappa_{21}\bar{p}_1 \left(2\kappa_{11} + \kappa_{12}\bar{p}_1 - \kappa_{14}\bar{p}_1^3 - 2\bar{p}_1^4\right)\left(\kappa_{22} + 2\kappa_{23}\bar{p}_2 + 3\kappa_{24}\bar{p}_2^2 + 4\bar{p}_2^3\right)}{(\kappa_{11} + \kappa_{12}\bar{p}_2 + \kappa_{13}\bar{p}_1^2 + \kappa_{14}\bar{p}_1^3 + \bar{p}_1^4)^2(\kappa_{21} + \kappa_{22}\bar{p}_2 + \kappa_{23}\bar{p}_2^2 + \kappa_{24}\bar{p}_2^3 + \bar{p}_2^4)^2} \cdot$$

Again, plus and minus signs are possible and as documented in figure 19 two bifurcations, the pitchfork bifurcation which is typical for cooperative **rep-rep** systems and a Hopf bifurcation are indeed observed.

Without showing details we mention that the Hopf bifurcation was not observed for all systems with regulatory determinants D that can have plus or minus sign. For example, no oscillations are observed in the systems transcribing $\mathsf{H}_1^{(4)}$ and 'intermediate 1' $\mathsf{H}_2^{(1)}$ or G_1 and 'intermediate 1' $\mathsf{H}_2^{(1)}$, respectively. More examples are listed in table 5. The situation in these cases is analogous to the activation-repression system with Hill coefficient $n = 2$: The regulatory determinant D adopts positive values but does not exceed $D = D_{\mathsf{Hopf}}$ for all tested values and approached limits.

5 Numerical sampling of parameter space

The results derived from selected examples are summarized and augmented by numerical explorations of parameter space in this section. Numerical sampling was performed in explorative manner in order to learn whether or not more complicated cases exist where the computer assisted analytic approach applied here is doomed to fail. For the sampling approach we assumed a constant total gene concentration of $g_0 = 1$ in problem adapted arbitrary units (See section 6). All rate and equilibrium parameters, $\pi_k, \; k = 1, 2, \ldots,$ were allowed to adopt values in the range $-9.25 \leq \log \pi_k \leq 9.25$ corresponding to approximately $10^{-4} \leq \pi_k \leq 10^4$. Individual values were sampled by means of a random number generator assuming uniform distribution on the logarithmic scale. A typical sample consisted of some ten thousand points and the distribution of different dynamical behaviors was evaluated by simple frequency counting. The results are summarized in tables 4 and 5. Despite relatively small samples all qualitative forms of dynamic behavior were detected by the numerical sampling procedure.

Table 4 presents also an overview over all activation and repression cases with simple Hill-type functions (5) for $n = 1, 2, 3,$ and 4. Basal activation or leaky transcription were also included. Almost all systems under consideration show an unregulated and a regulated regime separated by a bifurcation. The only exceptions are non-cooperative systems and the **act-rep** system with Hill coefficient $n = 2$.

Not all intermediate cases were investigated but the examples shown in table 5 are representative. They show transitions from one combination of basic regulatory scenario to another, for example from **act-rep** to **act-act** in the table. The pure combinations have their defined scenario, Hopf bifurcation and undamped oscillations for **act-rep** and one dimensional bifurcation and bistability for **act-act** and **rep-rep**. The intermediate cases form a smooth transition in the sense that they combine both scenarios, first one dimensional bifurcation and second Hopf bifurcation (One example combining both scenarios is shown in figure 18). The best studied and documented example is the case for Hill coefficient $n = 4$ in the table. All five objects from the naked gene to the complex with four monomers bound to DNA that can possibly initiate transcription are considered in the table. The pure systems show oscillations or bistability (with one state being the origin) and the intermediate complexes combine both behaviors – 'intermediate 1' and 'intermediate 2' – or they behave like the **act-act** system – 'intermediate 3'.

A very similar situation is encountered for the repression-intermediate system. We cannot give the details here, but figure 19 shows a parametric plot for one intermediate case, $\mathbf{G}_1$ and $\mathbf{H}_2^{(2)}$ that exhibits both, a one dimensional bifurcation leading to bistability with one state having one gene active and the other one silenced and the second state vice versa. Later, with increasing ϑ/K ratios one state becomes unstable and gives birth to a stable limit cycle via a Hopf bifurcation.

Table 4: Results of bifurcation analysis of systems with simple binding functions (5) **for activation and repression.** Equilibrium points were computed by means of equations (14) and the regulatory determinant D (21) was used for stability analysis.

Regulation $\mathbf{G}_1$			Regulation $\mathbf{G}_2$			Dynamical	Number of non-	Bifurcation
Type	$F_1(p_2)$	n_1	Type	$F_2(p_1)$	n_2	pattern[a]	negative roots[b]	type
activation	$\frac{p_2}{K_2+p_2}$	1	activation	$\frac{p_1}{K_1+p_1}$	1	E|S	1|2 (2)	transcritical
activation	$\frac{p_2}{K_2+p_2}$	1	repression	$\frac{K_2}{K_1+p_1}$	1	S	1 (2)	
repression	$\frac{K_2}{K_2+p_2}$	1	repression	$\frac{K_2}{K_1+p_1}$	1	S	1 (2)	
activation	$\frac{p_2^2}{K_2+p_2^2}$	2	activation	$\frac{p_1^2}{K_1+p_1^2}$	2	E|B(E,S)	1|3 (5)	saddle-node
activation	$\frac{p_2^2}{K_2+p_2^2}$	2	repression	$\frac{K_1}{K_1+p_1^2}$	2	S	1 (5)	
repression	$\frac{K_2}{K_2+p_2^2}$	2	repression	$\frac{K_1}{K_1+p_1^2}$	2	S|B(S$_1$,S$_2$)	1|3 (5)	pitchfork or saddle-node
activation	$\frac{p_2^3}{K_2+p_2^3}$	3	activation	$\frac{p_1^3}{K_1+p_1^3}$	3	E|B(E,S)	1|3 (9)	saddle-node
activation	$\frac{p_2^3}{K_2+p_2^3}$	3	repression	$\frac{K_1}{K_1+p_1^3}$	3	S|O	1|1 (9)	Hopf
repression	$\frac{K_2}{K_2+p_2^3}$	3	repression	$\frac{K_1}{K_1+p_1^3}$	3	S|B(S$_1$,S$_2$)	1|3 (9)	pitchfork or saddle-node
activation	$\frac{p_2^4}{K_2+p_2^4}$	4	activation	$\frac{p_1^4}{K_1+p_1^4}$	4	E|B(E,S)	1|3 (17)	saddle-node
activation	$\frac{p_2^4}{K_2+p_2^4}$	4	repression	$\frac{K_1}{K_1+p_1^4}$	4	S|O	1|1 (17)	Hopf
repression	$\frac{K_2}{K_2+p_2^4}$	4	repression	$\frac{K_1}{K_1+p_1^4}$	4	S|B(S$_1$,S$_2$)	1|3 (17)	pitchfork or saddle-node
basal+activation	$\gamma_1 + \frac{p_2}{K_2+p_2}$	1	basal+activation	$\gamma_2 + \frac{p_1}{K_1+p_1}$	1	S	1 (2)	
basal+activation	$\gamma_1 + \frac{p_2^2}{K_2+p_2^2}$	2	basal+activation	$\gamma_2 + \frac{p_1^2}{K_1+p_1^2}$	2	S|B(S$_1$,S$_2$)|S	1|3|1 (5)	saddle-node|saddle-node

[a] The sequence of states is obtained by increasing (k_1^Q, k_2^Q) at constant values of the other parameters, states are separated by \|, and the dynamical patterns are characterized by the following symbols: E $\equiv$ stable fixed point at the origin $\bar{P}(0,0)$ corresponding to both genes silenced, S $\equiv$ stable fixed point in the positive quadrant, $\bar{p}_1 > 0, \bar{p}_2 > 0$, B($\bar{P}_i, \bar{P}_j$) $\equiv$ two stable fixed points separated by a saddle, and O $\equiv$ limit cycle.

[b] Numbers of observed fixed points with $\bar{p}_1 \geq 0, \bar{p}_2 \geq 0$ before and after the bifurcations are separated by \|, the number in parentheses is the degree of the polynomial derived from equations (14). It is tantamount to the maximal number of fixed points.

Table 5: Results of numerical sampling of systems with randomly chosen parameter values.[a]

Regulation $\mathbf{G}_1$			Regulation $\mathbf{G}_2$			Dynamical	Bifurcation	Frequencies
Type	$F_1(p_2)$	n_1	Type	$F_2(p_1)$	n_2	pattern[b]	type	of patterns[b]
activation	$\frac{p_2^2}{\kappa_{21}+\kappa_{22}p_2+p_2^2}$	2	repression	$\frac{\kappa_{11}}{\kappa_{11}+\kappa_{12}p_1+p_1^2}$	0/2	S		1
activation	$\frac{p_2^2}{\kappa_{21}+\kappa_{22}p_2+p_2^2}$	2	intermediate	$\frac{\kappa_{12}p_1}{\kappa_{11}+\kappa_{12}p_1+p_1^2}$	1/2	E | B(E,S)	saddle-node	0.603|0.397
activation	$\frac{p_2^2}{\kappa_{21}+\kappa_{22}p_2+p_2^2}$	2	activation	$\frac{p_1^2}{\kappa_{11}+\kappa_{12}p_1+p_1^2}$	2/2	E | B(E,S)	saddle-node	0.663|0.337
activation	$\frac{p2^3}{\kappa_{21}+\kappa_{22}p_2+\kappa_{23}p_2^2+p2^3}$	3	repression	$\frac{\kappa_{11}}{\kappa_{11}+\kappa_{12}p_1+\kappa_{13}p_1^2+p1^3}$	0/3	S | O	Hopf	0.998|0.002
activation	$\frac{p2^3}{\kappa_{21}+\kappa_{22}p_2+\kappa_{23}p_2^2+p2^3}$	3	intermediate	$\frac{\kappa_{12}p_1}{\kappa_{11}+\kappa_{12}p_1+\kappa_{13}p_1^2+p1^3}$	1/3	E | B(E,S) | O	saddle-node | Hopf	0.642|0.354|0.004
activation	$\frac{p2^3}{\kappa_{21}+\kappa_{22}p_2+\kappa_{23}p_2^2+p2^3}$	3	intermediate	$\frac{\kappa_{13}p_1^2}{\kappa_{11}+\kappa_{12}p_1+\kappa_{13}p_1^2+p1^3}$	2/3	E | B(E,S) | O	saddle-node | Hopf	0.715|0.283|0.002
activation	$\frac{p2^3}{\kappa_{21}+\kappa_{22}p_2+\kappa_{23}p_2^2+p2^3}$	3	activation	$\frac{p1_3}{\kappa_{11}+\kappa_{12}p_1+\kappa_{13}p_1^2+p1^3}$	3/3	E | B(E,S)	saddle-node	0.720|0.280
activation	$\frac{p_2^4}{\kappa_{21}+\kappa_{22}p_2+\kappa_{23}p_2^2+\kappa_{24}p_2^3+p_2^4}$	4	repression	$\frac{\kappa_{11}}{\kappa_{11}+\kappa_{12}p_1+\kappa_{13}p_1^2+\kappa_{14}p_1^3+p_1^4}$	0/4	S | O	Hopf	0.988|0.012
activation	$\frac{p_2^4}{\kappa_{21}+\kappa_{22}p_2+\kappa_{23}p_2^2+\kappa_{24}p_2^3+p_2^4}$	4	intermediate	$\frac{\kappa_{12}p_1}{\kappa_{11}+\kappa_{12}p_1+\kappa_{13}p_1^2+\kappa_{14}p_1^3+p_1^4}$	1/4	E | B(E,S) | O	saddle-node | Hopf	0.673|0.321|0.006
activation	$\frac{p_2^4}{\kappa_{21}+\kappa_{22}p_2+\kappa_{23}p_2^2+\kappa_{24}p_2^3+p_2^4}$	4	intermediate	$\frac{\kappa_{13}p_1^2}{\kappa_{11}+\kappa_{12}p_1+\kappa_{13}p_1^2+\kappa_{14}p_1^3+p_1^4}$	2/4	E | B(E,S) | O	saddle-node | Hopf	0.740|0.258|0.002
activation	$\frac{p_2^4}{\kappa_{21}+\kappa_{22}p_2+\kappa_{23}p_2^2+\kappa_{24}p_2^3+p_2^4}$	4	intermediate	$\frac{\kappa_{14}p_1^3}{\kappa_{11}+\kappa_{12}p_1+\kappa_{13}p_1^2+\kappa_{14}p_1^3+p_1^4}$	3/4	E | B(E,S)	saddle-node	0.751|0.249
activation	$\frac{p_2^4}{\kappa_{21}+\kappa_{22}p_2+\kappa_{23}p_2^2+\kappa_{24}p_2^3+p_2^4}$	4	activation	$\frac{p_1^4}{\kappa_{11}+\kappa_{12}p_1+\kappa_{13}p_1^2+\kappa_{14}p_1^3+p_1^4}$	4/4	E | B(E,S)	saddle-node	0.742|0.258

[a] The frequencies of bifurcation patterns are derived from a large numbers ($N > 10\,000$) of randomly chosen combinations of parameters. The values for a parameter π are taken from the interval $-9.25 \le \log \pi \le 9.25$ under the assumption of a uniform distribution of $\log \pi$ (See also section 5).

[b] The sequence of states is obtained by increasing (k_1^Q, k_2^Q) at constant values of the other parameters, states are separated by \|, and the dynamical patterns are characterized by the symbols described in the footnote of table 4.

6   Discussion

The work reported here aims at the presentation of a straightforward and fairly simple mathematical technique that allows for full characterization of the dynamical patterns for gene regulation by transcription kinetics following equations (11) and (12). The procedure can be extended to investigations of the entire parameter space since, despite a rather large number of kinetic parameters and equilibrium binding constants, only very few quantities determine the dynamical pattern of the system – as encapsulated in the fixed points and their stabilities: Stationary mRNA concentrations (15) are proportional to stationary protein concentrations (14) and therefore it is sufficient to study the dynamical systems in the protein subspace. Moreover, the fixed points in protein space depend only on the binding function and one rational expression of kinetic parameters, $\vartheta_j = (k_j^{\mathrm{Q}} \cdot k_j^{\mathrm{P}})/(d_j^{\mathrm{Q}} \cdot d_j^{\mathrm{P}})$, for every gene. The stationary protein concentrations are obtained as solutions of polynomials. Since the polynomials are of high degrees for cooperative systems (Hill coefficient $n \geq 2$) a combined analytical and computational technique, consisting in the numerical calculation of the polynomial roots, is mandatory. Despite high degrees the polynomials allow for an analytical handling of limits like high and low binding affinities. Local stability analysis is performed in terms of the eigenvalues of the Jacobian matrix at fixed points.

In this contribution we presented examples for a (quite general) class of genetic regulations – denoted here as *simple* – where the analysis of the Jacobian is largely facilitated by its structure (21): Computation of the regulatory determinant D is sufficient for the stability analysis of fixed points. At two computable critical values, D_{oneD} and D_{Hopf}, the fixed points becomes unstable through a one dimensional bifurcation or a Hopf bifurcation, respectively. Fixed points are stable in between, $D_{\mathsf{oneD}} < D < D_{\mathsf{Hopf}}$. It is important for generalizations that D_{oneD} is always negative whereas D_{Hopf} has always positive sign. For two gene systems the class *simple* is constituted by cross-catalysis which expresses that regulatory binding functions depend only on the concentration of the protein derived from the other gene: $F_1(p_2)$ and $F_1(p_2)$. Apart from this restriction the binding functions can be arbitrarily complicated, only differentiability is required for the computation of D: Examples for more complicated cases analyzed here are leaky transcription (two terms) and intermediate complexes as transcription initiators.

The approach can be readily extended to more than two genes and there the properties of the class *simple* are fulfilled by catalytic cycles consisting of a closed loop of regulatory functions, $\mathsf{G}_N \Rightarrow \mathsf{G}_1 \Rightarrow \mathsf{G}_2 \Rightarrow \cdots \Rightarrow \mathsf{G}_N$ for arbitrary N. A description of such regulatory systems by means of dynamical graphs has been reported in [32]. One concrete example of a regulatory loop with $N = 3$ is the repressilator [15] which has been analyzed in detail (for example in [33]). On the other hand, there are also examples of two gene systems that do not fall under the classification *simple*, for example self-activation and cross-repression or self-repression and cross activation, because then the regulatory binding functions depend on the concentrations of both proteins: $F_1(p_1, p_2)$ and $F_2(p_1, p_2)$. Attempts to generalize our approach and to group these *non-simple* systems into subgroups according to the dynamical

structure related to the difficulty of analysis are under way [27].

The dynamical pattern of gene regulation has been analyzed for several cooperative binding functions, $F_1(p_2)$ and $F_2(p_1)$, with different Hill coefficients by means of a new technique using the regulatory determinant $D(p_1, p_2)$ introduced and defined in equation (21). We computed and classified only the generic dynamic features and the bifurcation patterns which were found in full agreement with the literature wherever previous studies were. No attempt has been made yet to make a complete search in parameter space, nor did we try in this paper to adjust to experimental data. Therefore concentrations and parameter values were chosen to illustrate best the basic features of the bifurcation diagrams and the oscillatory dynamics. A forthcoming study will deal with fitting regulatory dynamics to experimental data by making use of inverse methods [34, 35]. A particularly challenging problem is reverse engineering of bifurcation patterns for which first approaches are now available [36].

All cooperative systems (except activation-repression with Hill coefficient $n = 2$) show an unregulated and a regulated regime. The regulated regime is reached at sufficiently high values of the ratio ϑ/K implying that (i) transcription and translation are fast enough compared to mRNA and protein degradation, and (ii) binding is sufficiently strong. The *pure* systems[10] fall into three classes: **act-act**, **act-rep**, and **rep-rep**. Each class has its own regulatory characteristic, (i) **act-act** leads to both genes active or both genes silenced, (ii) **act-rep** results in oscillatory activity of the two genes, and (iii) **rep-rep** represents a bistable switch with the two states: (i) $\mathbf{G}_1$ active and $\mathbf{G}_2$ silenced, and vice versa (ii) $\mathbf{G}_1$ silenced and $\mathbf{G}_2$ active. In pure systems D is either always negative (**act-act** and **rep-rep**) or always positive (**act-rep**) and accordingly we find bistability only in the first two classes of systems and oscillations occur exclusively in the third class. More complicated binding functions may give rise to mixed behavior resulting from simultaneous appearance of one dimensional and Hopf bifurcations in the same bifurcation diagram. The cases of intermediate regulation discussed in section 4.2 may serve as examples.

The model for gene regulation and the technique to analyze regulatory dynamics presented here provides a fast tool for computational bifurcation analysis. The parameter spaces of small genetic networks with several genes can be scanned completely. Regulatory systems can be classified into *simple* and *non-simple* systems according to the structure of the Jacobian matrix. *Simple* systems are accessible to a highly efficient combined analytical and computational approach. Analytical expressions are available for the computation of bifurcation points. The current procedure will be developed further into an automatic tool for the exploration of entire parameter spaces that is applicable to systems with several genes (approximately up to five genes). Future work aims also at an upscaling to systems with many genes.

---

[10]The term *pure* indicates that the complex active in transcription is either fully saturated – $\mathbf{H}^{(4)}$ in figure 17 implying activation (**act**) – or unbound – $\mathbf{G}$ in figure 17 indicating repression (**rep**).

Acknowledgements

References

[1] J. Monod, J.-P. Changeaux, and F. Jacob. Allosteric proteins and cellular control systems. *J. Mol. Biol.*, 6:306–329, 1963.

[2] F. Jacob and J. Monod. Genetic regulatory mechanisms in the synthesis of proteins. *J. Mol. Biol.*, 3:318–356, 1961.

[3] B. C. Goodwin. Oscillatory behavior in enzymatic control processes. *Adv. Enzyme Reg.*, 3:425–439, 1965.

[4] J. Tiwari, A. Fraser, and R. Beckmann. Genetic feedback repression. I. Single locus models. *J. Theor. Biol.*, 45:311–326, 1974.

[5] J. J. Tyson and H. G. Othmer. The dynamics of feeback control circuits in biochemical pathways. *Prog. Theor. Biol.*, 5:1–62, 1978.

[6] H. Smith. Oscillations and multiple steady states in a cyclic gene model with repression. *J. Math. Biol.*, 25:169–190, 1987.

[7] R. Thomas and R. D'Ari. *Biological Feedback*. CRC Press, Boca Raton, FL, 1990.

[8] R. Thomas and M. Kaufman. Multistationarity, the basis of cell differentiation and memory. II. Structural conditions of multistationarity and other nontrivial behavior. *Chaos*, 11:180–195, 2001.

[9] M. A. Savageau. Design principles for elementary gene circuits: Elements, methods and examples. *Chaos*, 11:142–159, 2001.

[10] R. Albert and H. G. Othmer. The topology of the regulatory interactions predicts the expression pattern of the segment polarity genes in *Drosophila melanogaster*. *J. Theor. Biol.*, 223:1–18, 2003.

[11] D. A. Hume. Probability in transcriptional regulation and its implications for leukocyte differentiation and inducible gene expression. *Blood*, 96:2323–2328, 2000.

[12] J. L. Cherry and F. R. Adler. How to make a biological switch. *J. Theor. Biol.*, 203:117–133, 2000.

[13] M. Bindschadler and J. Sneyd. A bifurcation analysis of two coupled calcium oscillators. *Chaos*, 11:237–246, 2001.

[14] T. Kobayashi, L. Chen, and K. Aihara. Modeling genetic switches with positive feedback loops. *J. Theor. Biol.*, 221:379–399, 2003.

[15] M. B. Elowitz and S. Leibler. A synthetic oscillatory network of transcriptional regulators. *Nature*, 403:335–338, 2000.

[16] T. S. Gardner, C. R. Cantor, and J. J. Collins. Construction of a genetic toggle switch in *Escherichia coli*. *Nature*, 403:339–342, 2000.

[17] C. C. Guet, M. B. Elowitz, W. Hsing, and S. Leibler. Combinatorial synthesis of genetic networks. *Science*, 296:1466–1470, 2002.

[18] Y. Yokobayashi, R. Weiss, and F. H. Arnold. Directed evolution of a genetic circuit. *Proc. Nat. Acad. Sci.*, 99:16587–16591, 2002.

[19] M. Thattai and B. I. Shraiman. Metabolic switching in the sugar phophstransferase system of *Escherichia coli*. *Biophys. J.*, 85:744–754, 2003.

[20] L. H. Hartwell, J. J. Hopfield, S. Leibler, and A. W. Murray. From molecular to cellular biology. *Nature*, 402 (Supp):C47–C52, 1999.

[21] R. Thomas and M. Kaufman. Multistationarity, the basis of cell differentiation and memory. II. Logical analysis of regulatory networks in terms of feedback circuits. *Chaos*, 11:170–179, 2001.

[22] J. E. Ferrell. Self-perpetuating states in signal transduction:positive feedback, double feedback and bistability. *Curr. Opin. Cell. Biol.*, 14:140–148, 2002.

[23] M. Ptashne and A. Gann. *Genes & Signals*. Cold Spring Harbor Laboratory Press, Cold Spring Harbor, NY, 2002.

[24] P. Schuster. Binding of activators and repressors to DNA. Part I: Equilibria. Working Paper 05-05-016, Santa Fe Institute, Santa Fe, NM, 2005.

[25] C. K. Biebricher, M. Eigen, and W. C. Gardiner, Jr. Kinetics of RNA replication. *Biochemistry*, 22:2544–2559, 1983.

[26] C. K. Biebricher and M. Eigen. Kinetics of RNA replication by $Q\beta$ replicase. In E. Domingo, J. J. Holland, and e. P. Ahlquist, editors, *RNA Genetics I: RNA-directed Virus Replication.*, pages 1–21. Plenum Publishing Corporation, Boca Raton, FL, 1987.

[27] L. Endler, C. Flamm, and P. Schuster. Dynamic patterns of gene regulation II: Double regulatory functions and many gene interactions. Working paper, University of Vienna, Vienna, AT, 2005.

[28] A. V. Hill. The possible effects of the aggregation of the molecules of haemoglobin on its dissociation curve. *J. Physiology*, 40 [Section 11.2.1]: iv–vii, 1910.

[29] C. R. Cantor and P. R. Schimmel. *Biophysical Chemistry, Vol.I – III*. W. H. Freeman and Co., San Francisco, CA, 1980.

[30] M. Marcus. Two determinant condensation formulas. *Linear and Multilinear Algebra*, 22:95–102, 1987.

[31] I. Kovacs, D. S. Silver, and S. G. Williams. Determinants of commuting-block matrices. *Amer. Math. Monthly*, 106:950–952, 1999.

[32] E. Remy, B. Mossé, C. Chouiya, and D. Thieffry. A description of dynamical graphs asssociated to elementary regulatory circuits. *Bioinformatics*, 19, Suppl. 2:ii172–ii178, 2003.

[33] S. Müller, J. Hofbauer, L. Endler, C. Flamm, S. Widder, and P. Schuster. A generalized model of the repressilator. Working paper, University of Vienna, Vienna, AT, 2005.

[34] H. W. Engl, M. Hanke, and A. Neubauer. *Regularization of Inverse Problems – Mathematics and its Applications*. Springer-Verlag, Berlin, 1996.

[35] K. A. Woodbury, editor. *Inverse Engineering Handbook*. CRC Press, Boca Raton, FL, 2002.

[36] H. W. Engl, J. Lu, S. Müller, and P. Schuster. Inverse bifurcation analysis: Application to simple gene systems. *Bioinformatics*, 2006.

[37] F. R. Gantmacher. *The Theory of Matrices*, volume 2. AMS Chelsea Publishing, Providence, RI, 1998.

Appendix: Condition for a Hopf bifurcation

In order to compute the value D_{Hopf} (figure 2) where the two-gene system looses stability at positive values of D, we use the criterion by Liénard-Chipart (see [37], pp.221). According to that criterion, the eigenvalues of the Jacobian have strictly negative part if and only if the zeroth, second, and fourth coefficient of the secular equation as well as the second and fourth Hurwitz determinant are positive. The latter two are determinants of 2×2 and 4×4 matrices, respectively, whose nonzero entries are coefficient of the secular equation.

From equation (21), the zeroth and the second coefficient are always positive, and the fourth coefficient is positive for $D > -d_1^{\mathrm{Q}} d_2^{\mathrm{Q}} d_1^{\mathrm{P}} d_2^{\mathrm{P}}$. The second Hurwitz determinant is always positive because it expands to an expression in $d_1^{\mathrm{Q}}, d_2^{\mathrm{Q}}, d_1^{\mathrm{P}}, d_2^{\mathrm{P}}$ with positive coefficients. The fourth Hurwitz determinant is a quadratic polynomial in D. With the help of the computer algebra system Maple, one finds that it has two real roots, corresponding to the values

$$D_{\mathsf{trans}} = -d_1^{\mathrm{Q}} d_2^{\mathrm{Q}} d_1^{\mathrm{P}} d_2^{\mathrm{P}} \quad \text{and} \tag{23}$$

$$D_{\mathsf{Hopf}} = \frac{(d_1^{\mathrm{Q}} + d_2^{\mathrm{Q}})(d_1^{\mathrm{Q}} + d_1^{\mathrm{P}})(d_1^{\mathrm{Q}} + d_2^{\mathrm{P}})(d_2^{\mathrm{Q}} + d_1^{\mathrm{P}})(d_2^{\mathrm{Q}} + d_2^{\mathrm{P}})(d_1^{\mathrm{P}} + d_2^{\mathrm{P}})}{(d_1^{\mathrm{Q}} + d_2^{\mathrm{Q}} + d_1^{\mathrm{P}} + d_2^{\mathrm{P}})^2} \ . \tag{25}$$

Between these two roots it is positive because its leading coefficient is negative, the eigenvalues of the Jacobian have strictly negative real parts, and the corresponding fixed point is asymptotically stable.